Quaternary Science Reviews 114 (2015) 1–17

Contents lists available at ScienceDirect

Quaternary Science Reviews

journal homepage: www.elsevier.com/locate/quascirev

Invited review

Holocene evolution of the western Greenland Ice Sheet: Assessing geophysical ice-sheet models with geological reconstructions of ice-margin change

Nicolás E. Young [a, *], Jason P. Briner [b]

[a] Lamont-Doherty Earth Observatory of Columbia University, Palisades, NY 10964, USA
[b] Department of Geology, University at Buffalo, Buffalo, NY 14260, USA

ARTICLE INFO

Article history:
Received 30 August 2014
Received in revised form
15 January 2015
Accepted 20 January 2015
Available online

Keywords:
Greenland Ice Sheet
Ice-margin reconstructions
^{10}Be dating
Lake sediments
Holocene

ABSTRACT

Geophysical ice-sheet models are used to predict future ice-sheet dimensions and, in turn, these projections help estimate the magnitude of eustatic sea-level rise. Before models can confidently predict ice-sheet behavior, they must be validated by being able to duplicate the geological record of ice-sheet change. Here, we review geological records of Greenland Ice Sheet (GrIS) change, with emphasis on the warmer-than-present middle Holocene, and compare these records to published studies that numerically simulate GrIS behavior through the Holocene. Geological records are concentrated in West and Southwest Greenland, which are also the regions where the GrIS margin likely experienced the greatest distance of inland retreat during the middle Holocene. Several records spanning from Melville Bugt to Jakobshavn Isfjord in western Greenland indicate the GrIS achieved its minimum extent between ~5 and 3 ka, and farther south in the Kangerlussuaq region, new data presented here indicate the ice margin reached its minimum extent between ~4.2 and 1.8 ka. In the Narsarsuaq region in southern Greenland, the GrIS likely achieved its minimum configuration between ~7 and 4 ka. We highlight key similarities and discrepancies between these reconstructions and model results, and finally, we suggest that despite some degree of inland retreat, the West and Southwest GrIS margin remained relatively stable and close to its current position through the Holocene thermal maximum.

1. Introduction

The GrIS is the largest ice mass in the Northern Hemisphere with an estimated 7.36 m sea-level equivalent and is expected to be a key contributor to 21st century sea-level rise (Bamber et al., 2013). The recent Intergovernmental Panel on Climate Change Fifth Assessment Report projects that the GrIS contribution to global mean sea-level rise by AD 2100 will range between 7 and 21 cm with a median value of 12 cm under the RCP8.5 scenario (the strongest forcing scenario; Church et al., 2013), whereas an independent estimate ranges between 4.5 and 66.3 cm, with an average estimate of 22.3 cm over the next 100 years under conditions similar to the RCP8.5 scenario (Bindschadler et al., 2013). Estimates of GrIS-induced sea-level rise such as these are dependent upon numerical geophysical ice-sheet models of varying complexity (e.g. Nowicki et al., 2013), but regardless of complexity, models require some degree of "spin-up" or tuning to test model validity before forward modeling can commence. Within this framework, well-constrained geological records of GrIS change can provide important spatial and temporal benchmarks for which to test numerical ice-sheet models.

Decades of research have resulted in numerous reconstructions of GrIS dimensions through the late Pleistocene (e.g. Weidick, 1968; Ten Brink and Weidick, 1974; Hjort, 1981; van Tatenhove et al., 1996; Bennike and Björck, 2002; Weidick and Bennike, 2007; Larsen et al., 2014). The overwhelming majority of these records are reconstructions of the GrIS when it was larger than today, but there are a number of records providing constraints on a smaller-than-present GrIS (e.g. Weidick et al., 1990). In light of projected 21st century warming, which is likely to be amplified in the Arctic (Miller et al., 2010a; Collins et al., 2013), it is these reconstructions of a smaller-than-present GrIS that are most relevant for accurately predicting the dimensions of the GrIS, and thus estimating its future contribution to global mean sea-level rise.

* Corresponding author.
E-mail address: nicolasy@ldeo.columbia.edu (N.E. Young).

http://dx.doi.org/10.1016/j.quascirev.2015.01.018
0277-3791/

Although well-constrained geological records of a smaller-than-present GrIS are critical for predicting the GrIS' future dimensions in a warming world, it is extremely difficult to develop reliable and direct measures of a restricted GrIS. This difficulty arises primarily from the simple fact that following times of a smaller GrIS in the past, re-growth of the GrIS overran and destroyed any evidence on the landscape (e.g. moraines) that would help delimit the configuration of a reduced GrIS. Nonetheless, the dimensions of the GrIS during notable warm periods such as Marine Isotope Stage (MIS) 5e (~128–116 ka; the Last Interglacial) and the exceptionally long MIS 11 interglacial (~424–395 ka) remains a key focus within the paleoclimate community (Carlson et al., 2008; Colville et al., 2011; NEEM Community Members, 2013). Because of the difficulty in deciphering the dimensions of GrIS during past warm periods, indirect geological evidence is often used to infer the past dimensions of the GrIS. For example, reconstructed surface temperatures and ice-sheet elevations from MIS 5e-dated Greenland ice have been used to infer a relatively stable MIS 5e GrIS, and isotopic

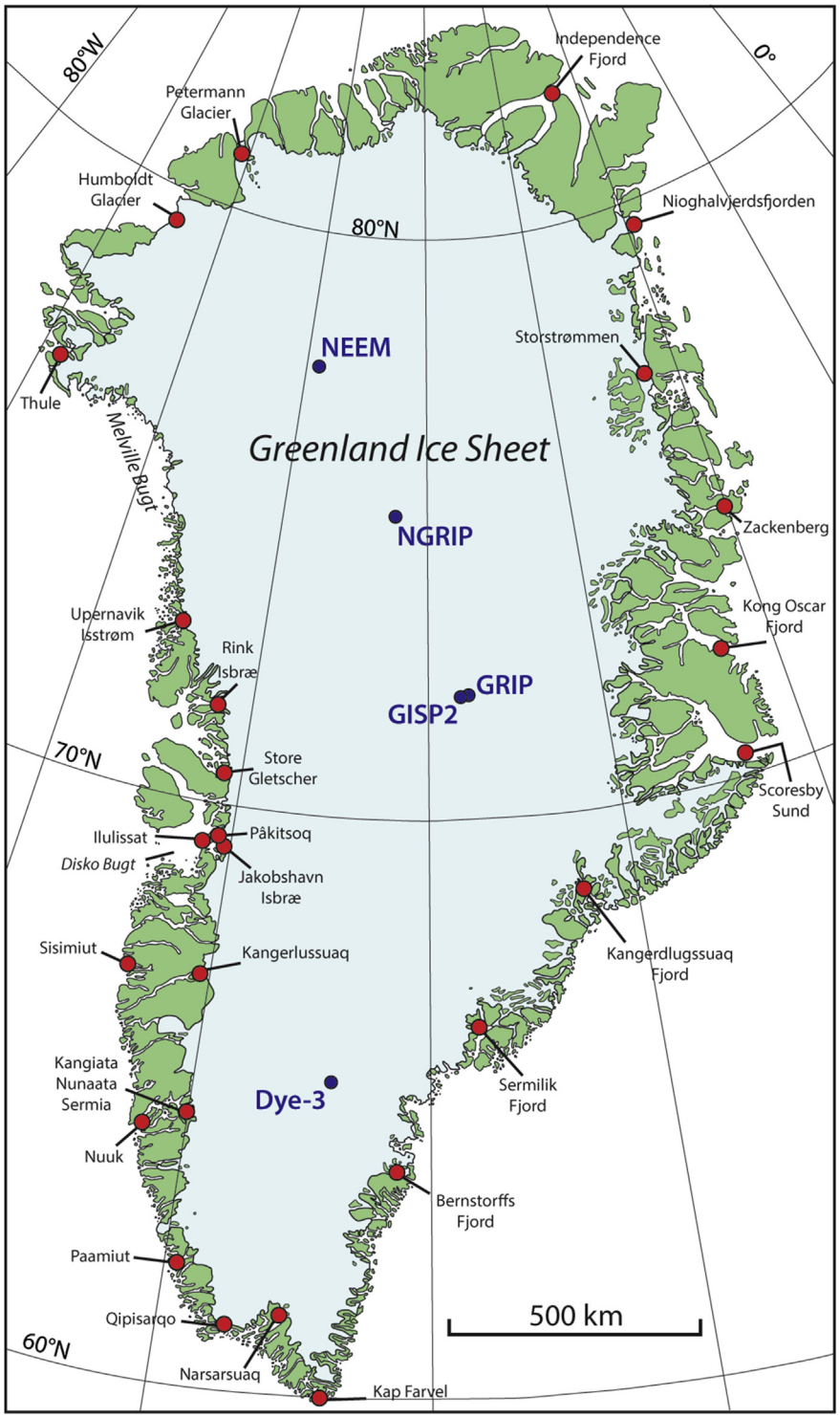

Fig. 1. Map of Greenland with locations discussed in the text.

Table 1
Summary of ages constraining final deglaciation in the early to middle Holocene.

Location/study	Age	Type	Notes	Reference
1	10,040 ± 210	^{10}Be	n = 2; supported by basal minimimum radiocarbon age 9550 ± 50 cal yr BP	Briner et al., 2013
2	7600 ± 310	^{10}Be	n = 12; subset of dataset that most directly relates to final deglaciation	Corbett et al., 2011
3	7740 ± 340	^{10}Be	n = 7	Carlson et al., 2014
4	7510 ± 220	^{10}Be	n = 7; supported by basal minimum radiocarbon ages of 7290 ± 20 and 7210 ± 40 cal yr BP	Young et al., 2013
4a	6500 ± 200	^{10}Be	n = 1	Young et al., 2013
5	6990 ± 130	^{10}Be	n = 2; supported by basal minimimum radiocarbon age 6750 ± 110 cal yr BP (Kelley et al., 2012)	Young et al., 2013
6	6810 ± 350	^{10}Be	n = 9; supported by 14C-based estimate of 6.8 ± 0.3 ka (van Tatenhove et al., 1996)	Levy et al., 2012
7	6950 ± 440	^{10}Be	n = 7; see comment above	Carlson et al., 2014
8	10,350 ± 120	^{14}C	Ua-3476; *Macoma calcarea*; 9490 ± 105 ^{14}C yrs BP; Bivalve reworked into a younger moraine	Weidick et al., 2012
9	10,170 ± 190	^{10}Be	n = 2	Larsen et al., 2014
10	10,330 ± 650	^{10}Be	n = 5	Larsen et al., 2014
11	10,690 ± 630	^{10}Be	n = 9	Carlson et al., 2014
12	9530 ± 30	^{14}C	CURL-4914; Bryophyte; 8560 ± 50 ^{14}C yrs BP; minimum age	Kaplan et al., 2002
13	11,110 ± 430	^{10}Be	n = 4	Carlson et al., 2014
14	10,430 ± 490	^{10}Be	n = 9; ages show no trend with distance up-fjord; mean of all erratics	Dyke et al., 2014
15	12,660 ± 1200	^{10}Be	n = 12; ages show no trend with distance up-fjord or elevation; stated value is mean of all ages	Roberts et al., 2008
16	10,910 ± 430	^{10}Be	n = 6; ages show no trend with distance up-fjord; mean of all erratics	Hughes et al., 2012
17	11,830 ± 1040	^{10}Be	n = 7; ages show no trend with distance up-fjord; mean of all erratics	Dyke et al., 2014
18	7820 ± 120	^{14}C	I-5421; *Mya truncata*; 6990 ± 130 ^{14}C yrs BP (7140); minimum age	Funder, 1978
19	7800 ± 70	^{14}C	Lu-1070; *Hiatella arctica*; 6980 ± 75 ^{14}C yrs BP (7530); minimum age	Håkansson, 1976
20	8050 ± 110	^{14}C	I-9104; *Mya truncata*, *Hiatella arctica*; 7210 ± 115 ^{14}C yrs BP (7360); minimum age	Weidick, 1977
21	8470 ± 120	^{14}C	I-9659; *Mya truncata*, *Hiatella arctica*; 7645 ± 125 ^{14}C yrs BP (7795); minimum age	Weidick, 1978
22	8110 ± 70	^{14}C	AAR-4703; *Portlandia arctica*; 7305 ± 65 ^{14}C yrs BP (7855); minimum age	Bennike and Weidick, 2001
23	7780 ± 160	^{14}C	UA-10557; *Hiatella arctica*; 6930 ± 170 ^{14}C yrs BP (7480); minimum age	Bennike and Weidick, 2001
24	7590 ± 80	^{14}C	HAR-3563; *Mya truncata*; 6730 ± 90 ^{14}C yrs BP (6730); minimum age	Funder, 1982
25	6270 ± 70	^{14}C	UA-4587; *Hiatella arctica*; 5480 ± 80 ^{14}C yrs BP (6030); minimum age	Landvik et al., 2001
26	6770 ± 120	^{14}C	HAR-6287; *Mya truncata*; 5930 ± 100 ^{14}C yrs BP (6480); minimum age	Kelly and Bennike, 1992
27	7560 ± 50	^{14}C	AAR-5762; *Mya truncata*; 6690 ± 65 ^{14}C yrs BP (7240); minimum age	Bennike, 2002
28	9730 ± 190	^{14}C	I-9691; *Hiatella arctica*; 8715 ± 140 ^{14}C yrs BP (8715); minimum age	Weidick, 1978
29	10,820 ± 230	^{10}Be	n = 3; three youngest ages of 28 total ages; see original reference for details of interpretation	Corbett et al., 2015
30	10,680 ± 380	^{14}C	I-9663; *Mya truncata*; 9385 ± 145 ^{14}C yrs BP (9385); minimum age	Weidick, 1978
31	9550 ± 130	^{14}C	K-3276; Gyttja; minimum age	Fredskild, 1985
32	9060 ± 60	^{14}C	LuS-6443; *Balaena mysticetus*; 8125 ± 50 ^{14}C yrs BP (8525); minimum age	Bennike, 2008
33	5160 ± 300	^{10}Be	n = 3	Lane et al., 2014
34	8730 ± 480	^{10}Be	n = 1; innermost ^{10}Be age from fjord-long transect	Roberts et al., 2013

^{10}Be ages and their uncertainties are rounded to the nearest decade.
The stated uncertainties for ^{10}Be-based age assignments include the analytical and ^{10}Be production-rate uncertainty. The stated uncertainty for the Baffin Bay ^{10}Be production rate is 1.8% for Lm scaling (Young et al., 2013a).
See Supplemental Table for ^{10}Be sample input information.
Calibrated ^{14}C ages are presented at 1σ uncertainty. Also provided is the uncalibrated reservoir-corrected ^{14}C age and the raw uncorrected ^{14}C age in parentheses.

measurements from Greenland-derived sediment in marine cores have been used to assess the magnitude of deglaciation of different sectors of southern Greenland during MIS 5e and 11 (Colville et al., 2011; NEEM Community Members, 2013; Reyes et al., 2014). Moreover, studies such as these are often coupled with ice-sheet model outputs in order to better assess their field-based reconstructions, and combined with further efforts that rely solely on numerical modeling to reconstruct GrIS behavior during past warm intervals (e.g. Otto-Bliesner et al., 2006; van de Berg et al., 2011), these studies highlight the critical importance in developing robust ice-sheet models.

The current interglacial period also presents an opportunity to assess the GrIS′ behavior in a warmer-than-present climate. Driven by higher Northern Hemisphere summer insolation through the early and middle Holocene, the Holocene thermal maximum in the Arctic was characterized by temperatures that were ~1–3 °C above 20th century averages and likely similar to those projected for AD 2100 (Kaufman et al., 2004; Miller et al., 2010b). In response to this warming, the GrIS retreated to a smaller-than-present configuration before re-expanding during the late Holocene (Funder et al., 2011). Whereas the magnitude of GrIS mass loss during the middle Holocene was almost certainly less than MIS 5e and MIS 11 mass loss, evaluating the middle Holocene configuration of the GrIS still provides valuable insights into ice-sheet behavior in a warming world and allows an assessment of the forcing mechanisms driving this behavior. Furthermore, it is more difficult to develop reliable ice-sheet reconstructions farther back in time and therefore it is more straightforward to develop early to middle Holocene ice-sheet reconstructions than from prior warm periods.

Here, we briefly review the deglaciation history of the GrIS and then provide an in-depth review of the early to middle Holocene geological record of GrIS change with a particular emphasis on the GrIS′ minimum configuration. Included in this review are new data from lake basins in the Kangerlussuaq region in Southwest Greenland that help constrain the timing and magnitude of the minimum extent of the GrIS. We compare these geological constraints to available ice-sheet model outputs covering the same period in order to identify consistencies and discrepancies between the two approaches.

2. Overview

This paper's focus is on geological records that are directly linked to the GrIS (Fig. 1), but we recognize that relative sea-level histories derived from isolation basins around Greenland have helped constrain Holocene fluctuations of the GrIS (e.g. Long et al., 2006). Some of these records are mentioned in our discussion, but we direct interested readers to Long et al. (2011). Finally, it is worth noting that records of early to middle Holocene GrIS change are more concentrated in West and Southwest Greenland. West and Southwest Greenland benefit from hosting several of Greenland's major towns (e.g. Nuuk and Ilulissat) and logistical hubs (e.g. Kangerlussuaq and Thule Air base) making fieldwork in these regions less logistically challenging than fieldwork in the more remote areas of eastern and northern Greenland.

Early through late Holocene geological records considered here fall into three chronological categories: 1) the timing of when the ice-sheet margin retreated behind its current limit in the early or middle Holocene, 2) the duration of when the ice margin was behind its current margin, including the timing of its minimum extent, and 3) the timing of when the ice margin approached and then reached its late Holocene maximum extent. The timing of when the ice margin first retreated behind its current margin during early to middle Holocene deglaciation is typically constrained by either basal radiocarbon ages from lake basins, ^{10}Be surface exposure ages (^{10}Be ages) located just beyond the historical moraine (generally deposited sometime in the last few hundred years; see below), or radiocarbon ages from marine fauna within raised marine deposits near the current ice margin (Table 1). Radiocarbon ages reported here have been recalibrated using CALIB 7.0 and the IntCal13 calibration curve, and all ^{10}Be ages have been recalculated using the Baffin Bay ^{10}Be production rate and are discussed with 'Lm' scaling (Young et al., 2013a). Most of the ^{10}Be ages considered here were calculated with the northeastern North America production rate (NENA; Balco et al., 2009) in their original publication; because the Baffin Bay and NENA are very similar, recalculated ^{10}Be ages are similar to the original published ages. In addition, ^{10}Be-determiend age assignments discussed in the text include the Baffin Bay production-rate uncertainty propagated through (~1.8%). All of the necessary ^{10}Be input information is located in Supplementary Table 1 in the CRONUS-Earth online calculator appropriate format (http://hess.ess.washington.edu/; Balco et al., 2008).

The duration of when the GrIS margin was behind its current position is typically constrained to the period between when the ice margin retreated behind its current position in the early to middle Holocene and the age of the historical ice limit. In some regions the historical limit is characterized by a well-defined trimline, but in most places, the historical limit is expressed as a single moraine or several moraines that are fresh in appearance and generally unvegetated, but whose deposition is regionally asynchronous (Kelley et al., 2012). For this manuscript, we emphasize that the term 'historical moraine' does not carry a firm chronological age, except in regions where firm chronological constraints exist and are discussed. In general, we casually ascribe the historical moraine to the Little Ice Age (LIA; ~1450–1850 AD; Masson-Delmotte et al., 2013) meaning that the GrIS likely approached or reached its historical limit sometime during the LIA, and remained at that limit until, at least in some regions, the early 20th century.

Also constraining the total duration of when the GrIS margin was behind its current position are radiocarbon ages from marine fauna reworked into the historical moraine at marine-based sectors of the ice sheet (e.g. Weidick and Bennike, 2007). In this context, each individual radiocarbon age is interpreted as marking a time of retracted ice, thus facilitating open ocean water and the presence of marine fauna. Sediments from 'threshold' lakes also constrain the duration of smaller-than-present ice (e.g. Briner et al., 2010). These records rely on the typically sharp transition between organic and minerogenic sediments that reflect fluctuations of the ice margin into (minerogenic sediments), and out of (organic sediments) the lake's catchment, which in turn are dated with radiocarbon. Furthermore, radiocarbon-dated sediments from threshold lakes can constrain the timing of when the ice margin reaches its late Holocene maximum position, and any other periods when the ice margin may have approached its current position (see Sections 4.1–4.3).

3. Timing of retreat behind the current GrIS margin during the early to middle Holocene

In this section we briefly review the timing of Holocene deglaciation around the western and southwestern GrIS periphery and provide a series of ages that provide close constraints on when the ice margin first retreated behind its current margin in the early to middle Holocene. A number of chronological constraints exist from eastern and northern Greenland that limit the timing of deglaciation, but our primary focus is the western and southwestern GrIS discussed below. While not explicitly discussed in this section, the available constraints from eastern and northern Greenland are provided in Fig. 2 and Table 2. See Fig. 2 and Table 2 for individual details and a list of appropriate references.

3.1. West Greenland: Melville Bugt to Kangerlussuaq

In the Melville Bugt region (Fig. 1) very little ice-free land presently exists, and accordingly, the terrestrial deglacial chronology in this region is limited. In northern Melville, radiocarbon ages of 10.7, 9.6 and 9.1 cal ka BP provide minimum constraints on the timing of deglaciation (Weidick, 1978; Fredskild, 1985; Bennike, 2008), and also act as the closest constraints on when ice in this region retreated behind its current margin (Table 1; see discussion below). Supporting these ages are recent ^{10}Be ages from near Thule that constrain initial deglaciation to 10.8 ka (Corbett et al., 2015). To the south in the Upernavik Isstrøm region (Fig. 1), a radiocarbon age of 10.3 cal ka BP from basal lake sediments acts as a minimum age for regional deglaciation (Bennike, 2000), and six ^{10}Be ages at the Upernavik coast reveal that this area deglaciated at 11.5 ka (Corbett et al., 2013). At Disko Bugt and Jakobshavn Isfjord (Fig. 1), the GrIS retreated through the bay at ~10.8 ka and made landfall at 10.2 ka based on numerous ^{10}Be ages at the western fjord edge (Corbett et al., 2011; Young et al., 2011a, 2011b; Kelley et al., 2013), whereas the southern edge of Disko Bugt deglaciated slightly later at 9.2 ka (Kelley et al., 2013). Near Sisimiut to the south, a minimum constraining age of ~10.8 cal ka BP marks the timing of initial ice-margin retreat out of the ocean (Bennike et al., 2011). Following the transition from a predominantly marine-to terrestrial-based ice sheet between Jakobshavn Isfjord and Kangerlussuaq, continued ice-margin retreat was interrupted by deposition of the Fjord Stade moraines in the Jakobshavn Isfjord region 9.2 and 8.2 ka (Young et al., 2011b, 2013b), and deposition of the Taserqat, Sarfartôq-Avatdleq, Fjord and Umîvît-Keglen moraine systems between ~9.3 and 7.3 ka between Sisimiut and Kangerlussuaq (Ten Brink, 1975; Weidick, 1976; van Tatenhove et al., 1996).

At Upernavik, ^{10}Be ages (n = 2) from directly outboard of the historical moraine indicate that the GrIS retreated behind its present position at 10.0 ka (Fig. 2; Briner et al., 2013), which is supported by a minimum constraining basal lake radiocarbon age of

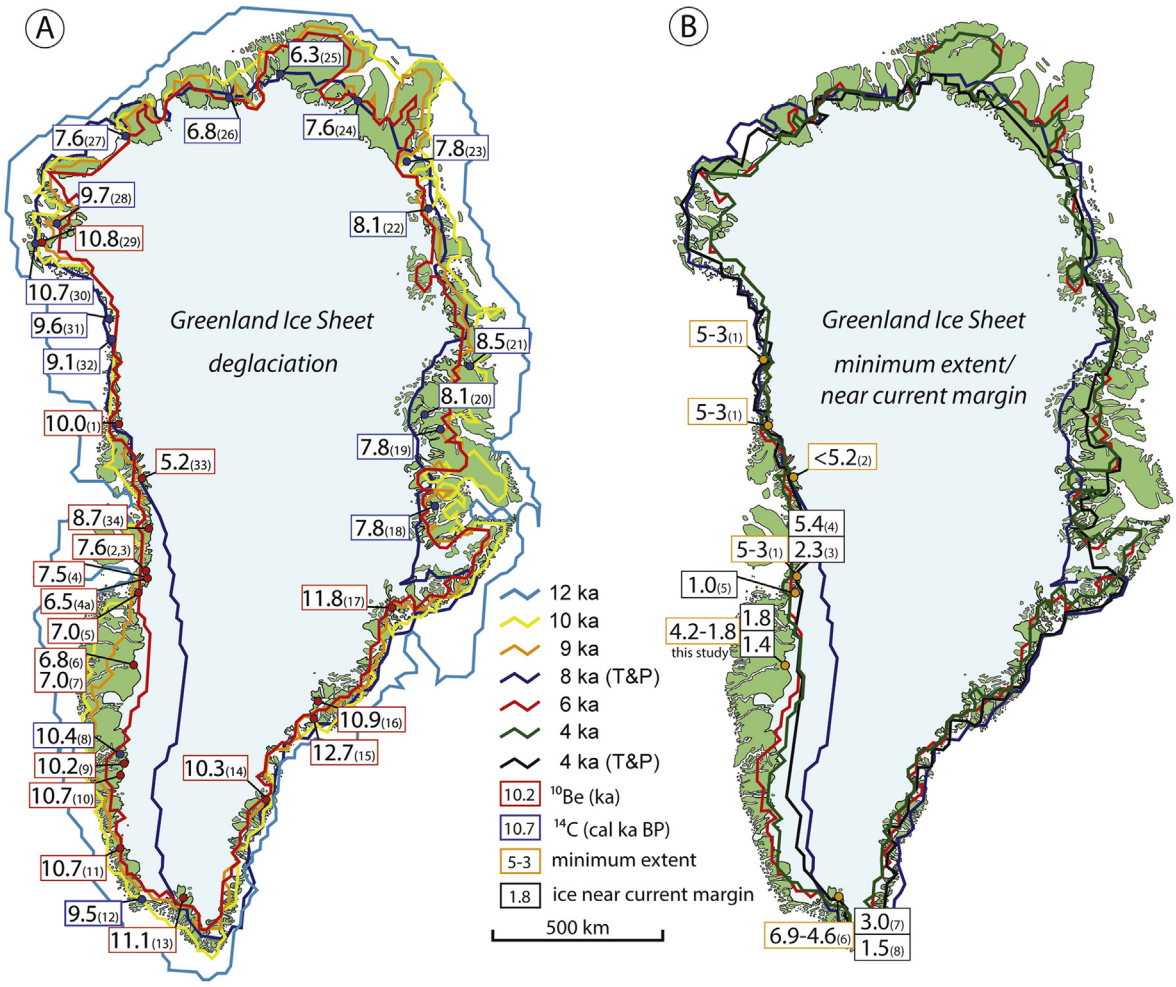

Fig. 2. A) Published ages constraining the timing of when the GrIS margin retreated behind its historical limit in the early to middle Holocene. These ages are compared to the modeled evolution of the GrIS from Lecavalier et al. (2014). For comparison, we also show the simulated ice margins at 8 and 4 ka from and Tarasov and Peltier (2003). Reference numbers are linked to Table 1. B) Published ages that estimate when the GrIS margin achieved its minimum Holocene extent and when the ice-sheet margin may have been near its current margin at times following the middle Holocene minimum, but before the LIA. Ages are compared to the modeled evolution of the GrIS margin from Lecavalier et al. (2014) and Tarasov and Peltier (2003). Reference numbers are linked to Table 2.

~9.6 cal ka BP (Table 1; Briner et al., 2013) and 4 additional ^{10}Be ages near the ice margin that range from 13.6 to 10.6 ka (Corbett et al., 2013). South of Upernavik at Rink Isbræ (Fig. 2), ^{10}Be ages (n = 3) located ~20 km down-fjord of the current ice margin indicate that following initial deglaciation of the region, ice lingered in the fjord until ~5.2 ka before retreating either close to or behind its current margin (Lane et al., 2014). And farther south at Store Gletscher, the ice margin likely reached its current margin by ~8.7 ka based on a single ^{10}Be age near the present ice margin (Roberts et al., 2013). At Pâkitsoq just north of Jakobshavn Isfjord (Figs. 2 and 3), seven ^{10}Be ages indicate that the landscape immediately outboard of the historical moraine deglaciated 7.7 ka (Fig. 3; Carlson et al., 2014). At Jakobshavn Isfjord, ^{10}Be ages from just outboard of the historical moraine constrain local deglaciation to 7.5 ka (Fig. 3; Young et al., 2013b), and additional ^{10}Be ages immediately north of the Jakobshavn Isfjord in Sikuijuitsoq Fjord (a tributary of the main Isfjord) constrain deglaciation to 7.6 ka (Corbett et al., 2011). Moreover, the ^{10}Be-based deglaciation age of 7.5 ka at Jakobshavn Isfjord is supported by minimum constraining radiocarbon ages of 7.3 and 7.2 cal ka BP from basal lake sediments just beyond the historical moraine (Table 1; Briner et al., 2010; Young et al., 2011a). On the south side of Jakobshavn Isfjord a single ^{10}Be age of ~6.5 ka is ~1 kyr younger than all remaining ^{10}Be ages in region (Fig. 3), and may reflect delayed deglaciation of this region. At the southern edge of Disko Bugt, two ^{10}Be ages from immediately outboard of the historical limit date to ~7.0 ka, which is supported by a minimum-constraining radiocarbon age of ~6.8 cal ka BP from basal lake sediments (Fig. 2; Kelley et al., 2012; Young et al., 2013b). Finally, the Ørkendalen moraines, which rest at the ice margin near Kangerlussuaq and are cross-cut by the historical ice limit, are dated with ^{10}Be to ~6.8 ka (n = 9; Levy et al., 2012) and ~7.0 ka (n = 7; Carlson et al., 2014). These ^{10}Be ages are supported by a minimum estimate of ~6.8 cal ka BP for deposition of the Ørkendalen moraines based on several radiocarbon ages in the region (Table 2: van Tatenhove et al., 1996).

3.2. Southwest Greenland: Nuuk to Cape Farewell

In Southwest Greenland near Nuuk (Fig. 1) radiocarbon-dated marine sediments indicate that the coast became ice free before 11.4 cal ka BP (Bennike and Björck, 2002; Larsen et al., 2014). Following deglaciation of the outer coast, the GrIS experienced brief stillstands or readvances during deposition of the Kapisigdlit stage moraines sometime between ~10.4 and 10.1 ka (Larsen et al., 2014). The outer coast at Kap Farvel was deglaciated by ~14.1 cal ka BP based on a minimum constraining radiocarbon age from basal lake

Table 2
Summary of constrains on the minimum ice extent or when ice is near its current margin.

Location/study (Fig. 2B)	Timing of likely minimum/timing of ice near current margin	Notes	Reference
1	5–3 cal ka BP	Age is derived from the peak in aspartic-acid-isomer-inferred (Asp) bivalve ages. The calibration curve used to derive Asp-based bivalve ages is constrained by 20 radiocarbon ages. Bivalves have been re-worked into the historical moraine and each bivalve age marks a time of smaller-than-present ice. See Briner et al. (2014) for full details.	Briner et al., 2014
2	<5.2 ka	^{10}Be ages from Rink-Karrat Fjord located ~20 km down-fjord from the current Rink Isbræ margin. Marks the timing of deglaciation and marks a time when the ice margin cannot be inland of its current position.	Lane et al., 2014
3	2.3 cal ka BP	Radiocarbon age of 2250 ± 90 cal yr BP at the upper contact between organic (gyttja) and minerogenic lake sediments at Goose Lake (threshold lake). Since 2250 ± 90 cal yr BP, silt-laden GrIS meltwater has spilled into the lake catchment	Briner et al., 2010
4	5.4 cal ka BP	Following deglaciation of the Paakitsoq region north of Jakobshavn Isbræ ca 7.6 ka (Corbett et al., 2011; Carlson et al., 2014), ice likely remained near its current position until ~5.4 cal ka BP based on the stratigraphy at Lake Lo. Radiocarbon age of 5410 ± 90 at the contact between minerogenic-rich sediments overlain by gyttja.	Håkansson et al., 2014
5	1.0 cal ka BP	Radiocarbon age of 960 ± 20 cal yr BP at the upper contact between organic and minerogenic sediments at Kuussuup Tasia (threshold lake). Radiocarbon age is from bulk sediment and may be slightly too old.	Kelley et al., 2012
This study	4.2–1.8 cal ka BP	Radiocarbon dated lake sediments from Lake Lucy suggest that following regional deglaciation ca 6.8–6.9 ka (Levy et al., 2012), the ice margin remained within 900 m of its current position until ~4.2 ka and has also been within 900 m of its current position over the last ~1.8 cal ka BP.	This study
6	6.9–4.6 cal ka BP	Following deglaciation of the region ~11.1 ka (Carlson et al., 2014), ice remained near its current margin until ~6.9 cal ka BP, and achieved its minimum extent sometime between ~6.9 and 4.6 cal ka BP based on radiocarbon ages and core stratigraphy at Lower Nordbosø (threshold lake) and the Narsaq Sound.	Nørgaard-Pedersen and Mikkelsen, 2009; Larsen et al., 2011
7	3.0–2.8 cal ka BP	Minerogenic sediments deposited ~3.0 cal ka BP in Lower Nordbosø lake indicating that the ice margin was near its current position at this time	Larsen et al., 2011
8	1.5 ka	^{10}Be ages (n = 10) from the Narsarsuaq moraine, which is located outboard of the historical moraine. The ^{10}Be-based age is supported by a minimum constraining radiocarbon age of ~1.2 cal ka BP from a lake impounded by the Narsasuaq moraines.	Bennike and Sparrenbom, 2007; Winsor et al., 2014

sediments, and the fjord mouths near Qipisarqo and Narsarsuaq were likely deglaciated at ~12 ka (Sparrenbom, 2006).

Near the Kangiata Nunaata Sermia (KNS) margin east of Nuuk (Fig. 1), a radiocarbon age of ~10.4 cal ka BP from a bivalve reworked into the historic moraine provides a minimum age of deglaciation for the landscape just outboard of the historical limit (Weidick et al., 2012). This age is supported by ^{10}Be-based estimates of 10.2 and 10.7 ka from areas immediately south of the KNS system (Fig. 2; Larsen et al., 2014). At the ice margin near Paamiut (Fig. 1), nine ^{10}Be ages reveal that ice retreated behind its historical moraine ~10.7 ka (Carlson et al., 2014), and farther south at Qipisarqo a minimum constraining radiocarbon age from basal lake sediments just beyond the historical limit is ~9.5 cal ka BP (Kaplan et al., 2002). At the Narsarsuaq margin, four ^{10}Be ages constrain the timing of final deglaciation to 11.1 ka (Carlson et al., 2014).

4. Minimum extent of the GrIS during the middle Holocene

Next we detail existing records that constrain the duration of when the GrIS achieved its minimum Holocene extent, the magnitude of inland retreat and when the GrIS approached its late Holocene maximum limit. In almost all locations around the GrIS periphery, the GrIS remained behind its current position for the entire duration between the timing of deglaciation outboard of the historical moraine and the timing of deposition of the historical moraine (see Fig. 2 and Table 1). Thus, we focus our discussion on records that are able to more precisely constrain the GrIS' Holocene minimum extent, and times prior to deposition of the historical moraine that the GrIS margin may have approached, and in some cases reached or nearly reached the eventual historical limit (Fig. 2 and Table 2). Furthermore, in addition to reviewing published research, we present new data from the Kangerlussuaq region (Fig. 1) that help constrain middle Holocene fluctuations of the GrIS.

4.1. West Greenland: Melville Bugt to Jakobshavn Isfjord

Briner et al. (2014) suggested that the Melville Bugt, Upernavik Isstrøm and Jakobshavn Isfjord sectors of the GrIS all reached their minimum Holocene extents ~5–3 ka (Fig. 2B; Table 2). This age assignment is based on the distribution of shell ages reworked into the historical moraine at each location. Although the ages of reworked marine fauna have been used routinely in the past to identify periods of smaller-than-present ice extent around Greenland (e.g. Weidick et al., 1990), the Briner et al. (2014) dataset warrants further discussion based on its sample size and geographical consistency. Typically bivalves that have been reworked into the historical moraine are individually dated with radiocarbon, and with several radiocarbon ages at one location, a frequency distribution of radiocarbon ages may yield important insights into the timing of retracted ice extent. The drawback of this approach is the cost of numerous radiocarbon analyses, thus making it difficult to generate large populations of ages. To address

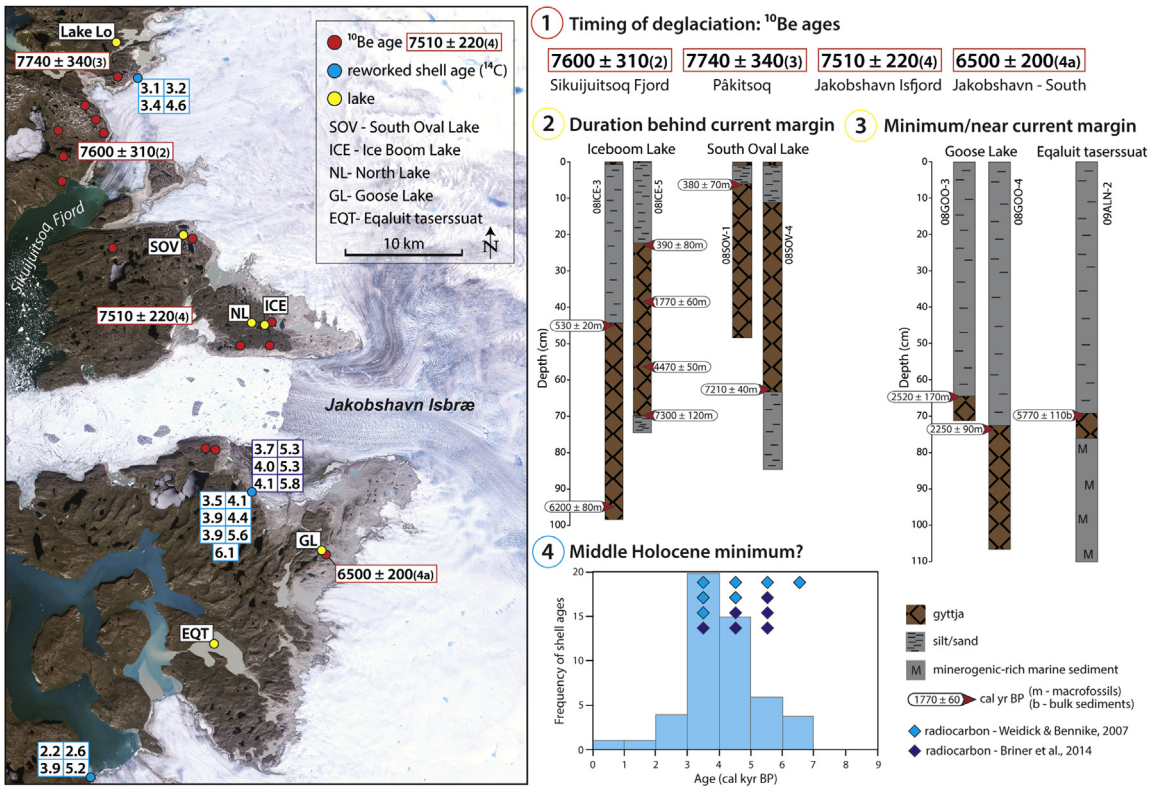

Fig. 3. Geological records at Jakobshavn Isfjord. 1) The timing of deglaciation outboard of the historical moraine constrained by ^{10}Be ages. Red dots are ^{10}Be age sample sites and the listed age is the mean ± s.d. of all samples for each dataset. Reference numbers are linked to Table 1. 2) and 3) Sediment records from threshold lakes that help constrain the duration of when the ice-sheet margin was behind its current margin and when the ice-sheet margin approached its historical extent prior to the LIA (Briner et al., 2010; Young et al., 2011a). 4) Distribution of aspartic acid inferred ages of shells reworked into the historical moraine that suggest this sector of the GrIS achieved its minimum extent ~5–3 ka (Briner et al., 2014). Radiocarbon ages of reworked shells (diamonds) are from Weidick and Bennike (2007; light blue) and Briner et al. (2014; dark blue). Basemap is a Landsat image from AD 2000.

this issue, Briner et al. (2014) measured enantiometric (D-isomers and L-isomers) separations of amino acids in 251 shell fragments of the bivalve *Mya Truncata* reworked into historical moraines. A subset of 20 samples that spanned the range of aspartic acid D/L values were then selected for radiocarbon dating and these ages were in turn used to develop a calibration curve and derive aspartic acid-inferred ages for all 251 original shell fragments. With this approach, histograms of aspartic-acid inferred ages all peak at ~5–3 ka in Melville Bugt, Upernavik Isfjord and Jakobshavn Isfjord and are interpreted as marking the timing of minimum ice extent at those three locations, albeit the magnitude of inland retreat is unknown. Although no firm constraints exist between Upernavik Isstrøm and Jakobshavn Isfjord that limit the timing or magnitude of the GrIS′ minimum extent, deglaciation and the minimum Holocene extent at Rink Isbræ must have occurred after ~5.2 ka (Fig. 2A and B; Lane et al., 2014), which is consistent with the aspartic-acid inferred Holocene minimum at Melville Bugt and Upernavik Isfjord. Moreover, these estimates are supported by a lake sediment record from Pâkitsoq just north of Jakobshavn Isfjord indicating that after initial deglaciation, ice remained near its present position until ~5.4 ka (Håkansson et al., 2014).

In addition to the distribution of reworked bivalve ages at Jakobshavn Isfjord (Fig. 3; Weidick and Bennike, 2007; Briner et al., 2014), a number of independent records help constrain the timing and magnitude of the GrIS′ minimum extent in the region. A series of threshold lakes in the Jakobshavn Isbræ forefield have been used to help constrain the Holocene history of the ice margin (Fig. 3; Briner et al., 2010; Young et al., 2011a). Radiocarbon-dated sediments from Iceboom and South Oval lakes, which currently do not receive silt-laden GrIS meltwater, reveal that following deglaciation ~7.5 ka the ice margin remained behind its current extent until 400 cal yr BP (Fig. 3). However, because of each lake's small drainage catchment, Iceboom and South Oval lakes only receive meltwater when the GrIS is near its late Holocene maximum. In contrast, radiocarbon-dated sediments from threshold lakes that currently receive GrIS meltwater reveal a more complete history of ice-margin change because these lake catchments currently extend under the GrIS. South of the Isfjord at Goose Lake, radiocarbon ages from the uppermost contact between organic and minerogenic sediments reveal that the GrIS has been within the lake catchment since shortly after ~2.3 cal ka BP (Briner et al., 2010; Fig. 3). Moreover, a single ^{10}Be age of ~6.5 ka from meters outboard of the historical margin near Goose Lake suggests that the broader ice margin must have achieved its minimum extent after ~6.5 ka. In Eqaluit Taserssuat, a large proglacial lake south of the Isfjord, a thin unit of organic sediment is bracketed by minerogenic-rich marine sediments below and minerogenic-rich lacustrine sediments above. A single radiocarbon age from bulk sediments near the upper contact organic-minerogenic contact suggests that the GrIS has remained within Eqaluit Taserssuat's catchment since ~5.8 cal ka BP (Fig. 3). However, because this single age is based on bulk sediments, the chronology of events is tenuous.

The precise magnitude of inland ice-margin retreat at Jakobshavn Isfjord is unknown. Weidick et al. (1990) suggested that this sector of the GrIS retreated ~15 km inland of its historical margin during the middle Holocene. Although it is unknown how far Eqaluit Taserssuat's catchment extends beneath the current GrIS, its sediments suggest that this sector achieved its minimum extent

~6–5 cal ka BP, and that the ice margin readvanced and was near its late Holocene maximum limit as early as ~2.3 cal ka BP based on dated sediments from Goose Lake (Fig. 3; Briner et al., 2010). In summary, the collection of lake sediment records and reworked marine fauna indicate that this sector of the GrIS reached its minimum extent after ~6–5 ka and before 2.3 ka.

4.2. West Greenland: Kangerlussuaq

Whereas the timing of middle Holocene deglaciation of the landscape immediately outboard of the historical moraine is well constrained to 7.0–6.8 ka (van Tatenhove et al., 1996; Levy et al., 2012; Carlson et al., 2014), comparatively little is known about the middle Holocene history of the ice margin in this region. Based on eolian activity in this region, Willemse et al. (2003) suggested that the GrIS was >15 km inland of its current position between ~3400 and 540 cal yr BP. However, Forman et al. (2007) presented optically stimulated luminescence ages from loess capping a moraine and suggested that the GrIS reached its present margin at ~2 ka.

4.2.1. New constraints in the Kangerlussuaq region: Lake Lucy and Sports Lake

We collected sediment cores from Lake Lucy (67.151°N, 50.123°W; 5.4 m water depth) and Sports Lake (67.132°N, 50.094°W; 3.4 m water depth) in 2009 and 2013 (Fig. 4). Lake Lucy and Sports Lake (informal names) are threshold lakes located <1 km from the GrIS margin; Lake Lucy currently receives silt-laden GrIS meltwater (it is a proglacial lake) whereas Sports Lake is currently dominated by organic sedimentation (Fig. 4). Lake Lucy has two inflows on the northeast and northwest sides of the lake that receive lateral meltwater off Insunnguata Sermia (Fig. 4), and a single outflow on its southern end. Sports Lake is currently a closed-basin lake, but when the ice-dammed lake immediately to the northeast is within ~1 m of its maximum lake level, the ice-dammed lake overflow spills into Sports Lake. This overflow raises the water level in Sports Lake forming an outflow at the southwest end of the lake. Thus, Sports Lake only receives silt-laden meltwater when the ice-dammed lake is at its maximum elevation (Fig. 4).

At Sports Lake, minerogenic sediments deposited during deglaciation are overlain by organic sediments followed by a thin minerogenic layer, a thick organic section, and two thin minerogenic layers (separated by a thin organic layer) in the uppermost ~5 cm (Fig. 5). At the base of the Sports Lake sediment package is a radiocarbon age of 6255 ± 40 cal yr BP and a radiocarbon age of 5840 ± 75 cal yr BP is from just above the thin minerogenic layer (Table 3; Fig. 5). The contact between the primary organic section and the first of the two uppermost minerogenic sediment layers is dated to 870 ± 65 cal yr BP and an additional radiocarbon age from between the uppermost minerogenic units has a modern solution (Table 3; Fig. 5). We note that at two depths we obtained indistinguishable radiocarbon ages from aquatic macrofossils and bulk sediments (Table 3) thereby indicating that radiocarbon ages from bulk sediments can yield reliable radiocarbon ages in this region. However, despite the coherency between macrofossil- and bulk sediment-derived radiocarbon ages, we suspect that the 870 ± 65 cal yr BP age from 4.5 cm depth is slightly too old after considering its down-core depth (4.5 cm) and that a radiocarbon age from 1.5 cm above yielded a modern solution. Alternatively, it is possible that the base of this minerogenic layer is an erosional contact with the underlying gyttja that formed with a sudden influx of GrIS meltwater; this too would result in a radiocarbon age that is older than the true age of the minerogenic layer. Regardless, we consider the 870 ± 65 cal yr BP age a maximum-limiting age on the minerogenic layer.

At proglacial Lake Lucy, deglacial minerogenic sediments are overlain by organic sediments, followed by ~30 cm of alternating

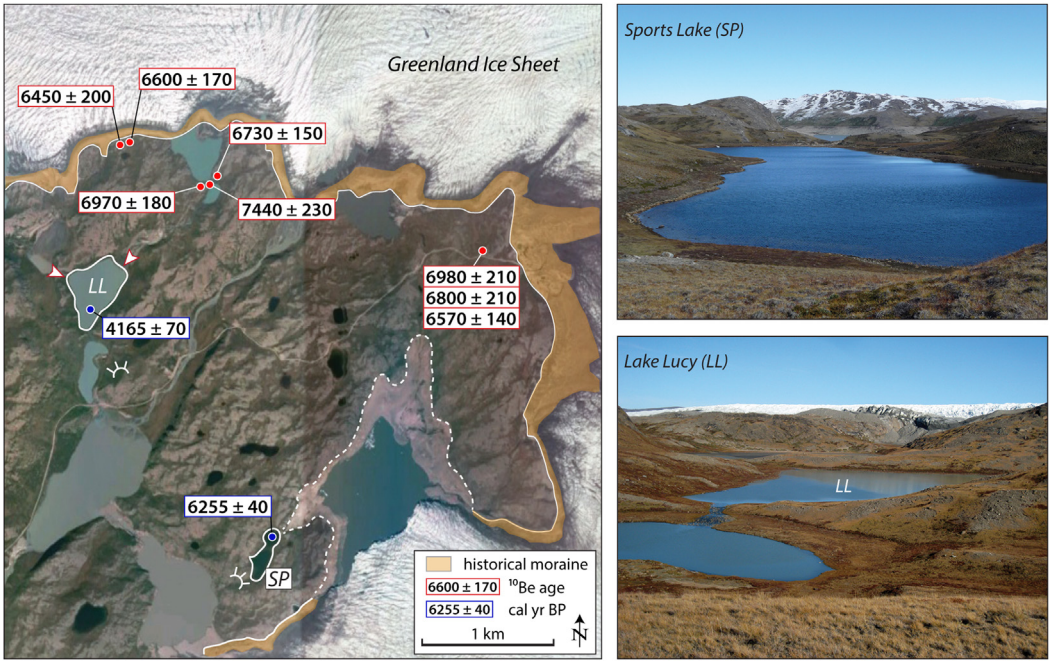

Fig. 4. Ice margin in the Kangerlussuaq region. Shown are ^{10}Be ages from Levy et al. (2012; western set of ages) and Carlson et al. (2014; eastern set of ages) that constrain local deglaciation to 7.0–6.8 ka. Levy et al. (2012) and Carlson et al. (2014) published 9 and 7 ^{10}Be ages, respectively, but we only show the ^{10}Be ages that fall within the map area. Also shown are the locations of Lake Lucy (LL) and Sports Lake (SP) with the basal radiocarbon age from each lake (Fig. 5). Arrows at LL are inflows. Also shown is the maximum level (dotted line) that must be achieved in order for SP to receive GrIS meltwater. The high lake level bathtub ring can be seen in the distance in the SP field photo. Base image is from Google Earth, AD 2012.

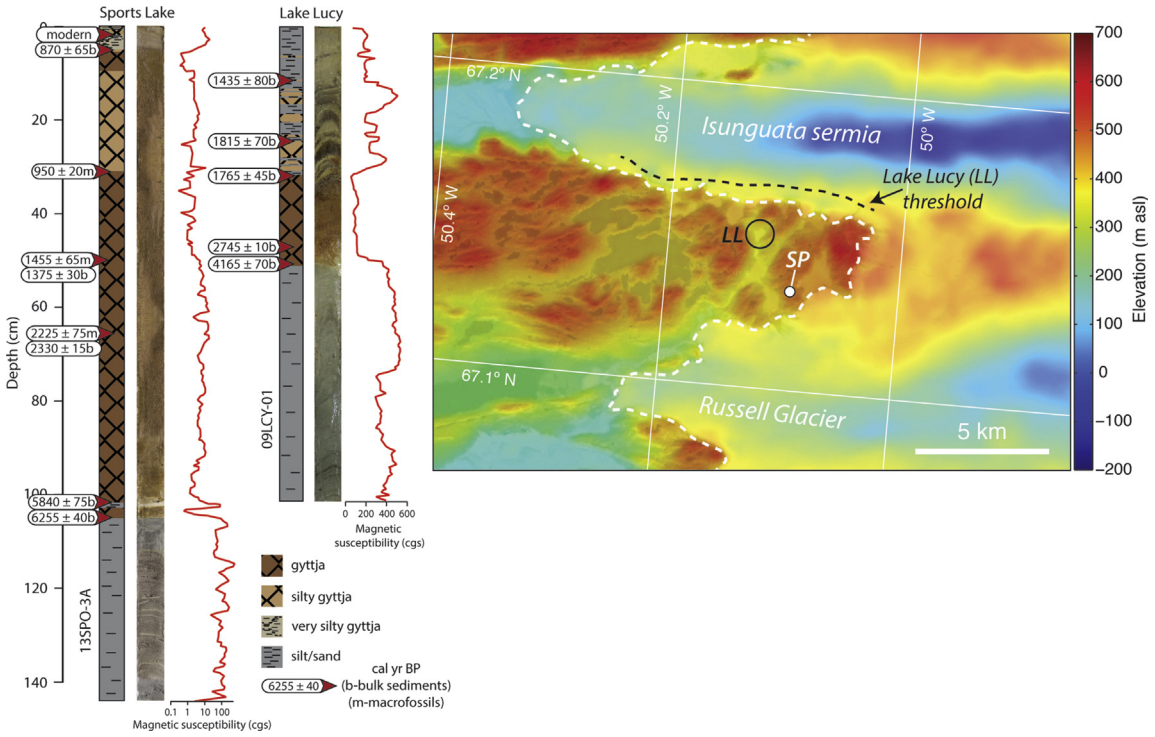

Fig. 5. Sediment records from Sports Lake and Lake Lucy shown with magnetic susceptibility profiles. Note that magnetic susceptibility values at Sports Lake are plotted on a log scale. Also shown is a map of the regional sub-ice topography (Morlighem et al., 2013). Highlighted is the topographic threshold resting ~900 m inland from the current ice margin that the ice sheet must cross in order for Lake Lucy to receive meltwater (dotted line). Sub-ice topography courtesy of M. Morlighem.

minerogenic and organic sediments (Fig. 5). A basal radiocarbon age is 4165 ± 65 cal yr BP; an age of 1765 ± 45 cal yr BP is from the contact between the primary organic unit and the first of several minerogenic layers. Seven cm above is a radiocarbon age of 1850 ± 70 cal yr BP, followed by our uppermost radiocarbon age of 1435 ± 80 cal yr BP (Table 3; Fig. 5).

The stratigraphy and chronology at Sports Lake is consistent with the idea that the GrIS achieved its maximum late Holocene limit sometime within the last millennium. The basal minimum age of 6255 ± 40 cal yr BP is consistent with the local deglaciation age of 7.0–6.8 ka derived from numerous ^{10}Be ages (Fig. 4). With the exception of a brief episode of minerogenic deposition ~5.8 cal ka BP, which we interpret to indicate a period of spillover from the ice-dammed lake and thus an ice position similar to today, the predominantly organic sediments of Sports Lake suggest that the ice margin was behind its current margin from ~5.8 cal ka BP until sometime in the last millennium.

The stratigraphy and chronology at proglacial Lake Lucy provide a complimentary record to Sports Lake. The minimum constraining basal age in Lake Lucy of ~4.2 cal ka BP is significantly younger than the timing of local deglaciation constrained by ^{10}Be. We suggest that following local deglaciation the GrIS remained within Lake Lucy's catchment spilling meltwater into the lake until ~4.2 cal ka BP, and that the GrIS achieved its minimum extent between ~4.2 cal ka BP and ~1.8 cal ka BP based on Lake Lucy's stratigraphy. Although there is a possible age reversal in the upper portion of the Lake Lucy record (Fig. 5), we interpret the stratigraphy and radiocarbon ages to broadly indicate that following the GrIS′ minimum extent, the GrIS readvanced and has been within or near Lake Lucy's catchment for the last ~1.8 cal ka BP (Fig. 5). Thus, sediments from Sports Lake indicate that at no time between ~5.8 cal ka BP and the last millennium has the GrIS been in a configuration similar to today, whereas sediments from Lake Lucy suggest that the GrIS achieved its minimum extent between ~4.2 and 1.8 cal ka BP and that since ~1.8 cal ka BP the GrIS has been within or near the lake catchment.

We utilized a high-resolution map of the sub-ice topography in the Kangerlussuaq region to better characterize the Lake Lucy drainage basin and develop a more robust interpretation of the Lake Lucy stratigraphy. Morlighem et al. (2013) used a mass-conservation approach to develop a map of sub-ice topography at 60 m resolution beneath the broader Insunnguata Sermia and Russell Glacier ice margin (Fig. 5). The sub-ice topography in the region does indeed confirm that Insunnguata Sermia occupies a valley, and is also able to identify the topographic threshold that dictates the routing of meltwater from Insunnguata Sermia into Lake Lucy's catchment (Fig. 5). This threshold is ~900 m from the current ice margin indicating that only relatively minor changes in the position of the ice-sheet margin will result in the cessation of meltwater into Lake Lucy (Fig. 5). By combining the Lake Lucy stratigraphy and chronology with the regional sub-ice topography, we suggest that following local deglaciation ~7.0–6.8 ka, the Insunnguata Sermia was within ~900 m of its current position until ~4.2 cal ka BP before thinning/retreating behind the valley wall and topographic threshold. After achieving a minimum extent between ~4.2 and 1.8 cal ka BP at an unknown distance inland, the ice margin readvanced and likely remained within ~1 km of its current position since ~1.8 cal ka BP.

4.3. Southwest Greenland: Narsarsuaq

The history of the GrIS margin in the Narsarsuaq region is best constrained by a lake sediment record from Lower Nordbosø located near the current ice margin (Larsen et al., 2011). Lower Nordbosø is a threshold lake that is presently proglacial; once the ice margin retreats behind a topographic threshold (with an as-yet undetermined location), Lower Nordbosø is dominated by organic sedimentation. Even though the landscape outboard of the

Table 3
Radiocarbon sample information from Lake Lucy and Sports Lake.

Lake	Depth (cm)	Material dated	Fraction modern	Radiocarbon age (^{14}C yr BP)	Calibrated age (cal yr BP ± 1σ)	Calibrated age (cal yr BP ± 2σ)	δ^{13}C (‰PDB)	Lab number
Lake Lucy								
09LCY-01	16	Bulk sediment	0.8278 ± 0.0033	1520 ± 30	1435 ± 80	1430 ± 90	−26.47	OS-93081
	27	Bulk sediment	0.7903 ± 0.0034	1890 ± 35	1815 ± 70	1820 ± 95	−26.41	OS-93148
	34	Bulk sediment	0.7976 ± 0.0024	1820 ± 25	1765 ± 45	1730 ± 90	−26.19	OS-96150
	45	Bulk sediment	0.7236 ± 0.0028	2600 ± 30	2745 ± 10	2720 ± 5	−26.91	OS-96151
	50	Bulk sediment	0.6237 ± 0.0027	3790 ± 35	4165 ± 70	4150 ± 140	−27.15	OS-93150
Sports Lake								
13SPO-3	3	Aquatic macrofossil	1.0515 ± 0.0024	Modern	NA	NA	−27.70	OS-106896
	4.5	Bulk sediment	0.8841 ± 0.0030	990 ± 25	870 ± 65	880 ± 80	−24.72	OS-106736
	31	Aquatic macrofossil	0.8780 ± 0.0039	1040 ± 35	950 ± 20	985 ± 70	−33.52	OS-106735
	50	Bulk sediment	0.8307 ± 0.0032	1490 ± 30	1375 ± 30	1410 ± 105	−29.98	OS-106711
	50	Aquatic macrofossil	0.8225 ± 0.0030	1540 ± 30	1455 ± 65	1445 ± 80	−35.49	OS-106734
	66	Bulk sediment	0.7519 ± 0.0023	2290 ± 25	2330 ± 15	2270 ± 85	−29.03	OS-106463
	66	Aquatic macrofossil	0.7617 ± 0.0019	2190 ± 20	2225 ± 75	2225 ± 85	−33.88	OS-106822
	102	Bulk sediment	0.5290 ± 0.0017	5110 ± 25	5840 ± 75	5835 ± 85	−20.08	OS-106462
	105	Bulk sediment	0.5069 ± 0.0015	5460 ± 25	6255 ± 40	6255 ± 45	−17.69	OS-106461

Radiocarbon ages are calibrated using CALIB 7.0, which implements the IntCal09 calibration dataset (Stuiver et al., 2005; Reimer et al., 2009).
Calibrated ages are reported as the midpoints of 1- and 2-sigma calibrated age range; 1- and 2-sigma ranges include the extreme ends of each range.
Calibrated ages and uncertainties are rounded to the nearest half-decade.

historical limit in the Narsarsuaq region deglaciated ~11.1 ka (Fig. 2; Carlson et al., 2014), the Lower Nordbosø record reveals that ice remained within the lake catchment until ~6.9 cal ka BP (Larsen et al., 2011). Between ~6.9 and ~3.0 cal ka BP, the ice margin was situated outside of Lower Nordbosø's catchment, before a readvance is recorded by a minerogenic unit dated to 3.0–2.8 cal ka BP. This minerogenic unit is overlain by organic sediments that record a time of reduced ice extent, followed by a cap of minerogenic sediments beginning ~0.5 cal ka BP (Larsen et al., 2011). Collectively, the Lower Nordbosø record indicates that ice was near its current position from ~11.1 ka to 6.9 cal ka BP, at 3.0–2.8 cal ka BP, and since 0.5 cal ka BP. An ice-rafted detritus (IRD) record from the nearby Narsuaq Sound provides additional constraints on the relative position of the GrIS through the Holocene (Nørgaard-Pedersen and Mikkelsen, 2009). The IRD flux generally decreased from ~8.0–4.8 cal ka BP, supporting the progressive inland retreat of the GrIS, but also indicating that the ice margin was still relatively close to the present margin. Renewed IRD influx ~4.6, 3.6, 2.2, 1.1, 0.7 and 0.5 cal ka BP generally agrees with the Lower Nordbosø record (Larsen et al., 2011).

The Narsarsuaq moraines are located ~20 km south of Lower Nordbosø and have been the subject of great interest as these moraines rest well beyond the historical ice limit and are thought to date to the late Holocene. Bennike and Sparrenbom (2007) obtained a basal radiocarbon of ~1.2 cal ka BP from a lake impounded by the outer Narsarsuaq moraines, indicating moraine deposition prior to this time. More recently, Winsor et al. (2014) dated ice retreat from a Narsarsuaq moraine to 1.51 ± 0.11 ka based on 10 ^{10}Be ages from between the innermost Narsarsuaq recessional moraine and the historical limit. Taken together the basal radiocarbon and ^{10}Be ages confirm that the Narsarsuaq moraines were deposited before ~1.2–1.5 ka. Not only do the Narsarsuaq moraines represent a late Holocene ice extent that is significantly more extensive than the historical limit, but they likewise mark a time when this sector of the ice margin could not have been well inland of its current margin.

5. Discussion

5.1. The spatiotemporal pattern of Holocene deglaciation

Deglaciation ages around the GrIS periphery span ~7 kyr (Fig 2), but noticeable patterns emerge after considering each ice-sheet sector's ice-margin environment. The earliest deglaciation ages occur in southern Greenland at Narsarsuaq, Paamiut and the KNS region, with early deglaciation also occurring in the Melville Bugt to Upernavik Isstrøm region and the southeastern sector of the GrIS (Fig. 2). All of these regions are generally marine-based environments and/or are dominated by marine-terminating outlet glaciers, and the GrIS is not far inland from the continental shelf. Many of these outlet glaciers occupy deep troughs, some extending several 10s of km under the GrIS (e.g. Morlighem et al., 2014), making them susceptible to ice loss and ice-margin retreat via calving. Moreover, marine margins are also influenced by submarine melting, which has been shown to act as a significant source of contemporary mass loss (e.g. Holland et al., 2008; Rignot et al., 2010). Indeed, not only was the timing of deglaciation relatively early along the marine-dominated southeastern coast, but Dyke et al. (2014) suggested that the deglacial asynchrony between Bernstorffs, Sermilik and Kangerdlugssuaq Fjords (Fig. 2) was driven by the asynchronous timing of when the warm Irminger Current, which runs along the southeastern Greenland shelf, was able to access each region. In contrast to the deglacial chronology at many of Greenland marine-based sectors, deglaciation ages are significantly younger at notable terrestrial-based sectors such as the Kangerlussuaq region and northern Greenland (Fig. 2). At these locations, ice loss is driven almost exclusively through surface melt making it slower to ablate ice compared to marine-based regions influenced by marine processes addition to surface melt.

Along Southwest and West Greenland, Carlson et al. (2014) hypothesized that the deglaciation ages of Pâkitsoq (7.6 ka), Kangerlussuaq (7.0–6.8 ka), Paamiut (10.7 ka) and Narsarsuaq (11.1 ka) marked the first time that, on multi-century timescales, regional temperatures warmed above average late Holocene temperatures. An alternative hypothesis, however, considers the total distance between the Last Glacial Maximum (LGM)/late-glacial ice limit and the historical ice limit. The LGM ice margin off southern Greenland at Narsarsuaq was positioned on the shelf break only ~60 km off the modern coastline and ~150 km from the historical margin at Narsarsuaq. In contrast, the LGM limit west of the Sisimiut–Kangerlussuaq transect was likely ~250–300 km west of the historical limit. Thus, the ~4 kyr offset between the timing of deglaciation at Narsarsuaq and Kangerlussuaq could simply reflect the total distance of retreat since the LGM. Once post-LGM retreat began south of Narsarsuaq, the ice margin had comparatively less distance to travel before crossing behind the eventual position of

the historical limit compared to the same scenario for the ice margin along the Sisimiut–Kangerlussuaq transect. The timing of deglaciation at Jakobshavn Isfjord (~7.5 ka) is relatively late compared to other marine-based sectors, but the total distance between the historical moraine and the LGM limit at the shelf break to the west is ~375 km, which may have contributed to the timing of deglaciation at Jakobshavn Isfjord.

The timing of deglaciation around western and southwestern Greenland could also in part be explained by the magnitude of the GrIS' late Holocene readvance or the magnitude of inland retreat during the middle Holocene. For example, if the western and southwestern GrIS margins retreated in unison, but experienced varying degrees of late Holocene regrowth, areas with a more extensive late Holocene advance would re-occupy terrain that deglaciated earlier compared to areas of the ice sheet that experienced a late Holocene readvance of a lesser magnitude. In this scenario, basal radiocarbon ages from lake basins or ^{10}Be ages from just beyond the historical ice limit in regions with a more extensive late Holocene readvance would by systematically older than ages from just beyond the historical moraine in regions with a minimal late Holocene readvance of the ice margin. Indeed, Briner et al. (2013) presented an example of this concept using the Jakobshavn Isfjord deglaciation chronology. Here, the historical moraine borders a landscape that deglaciated ~7.5 ka, beyond which rests the Fjord Stade moraines (9.3 and 8.2 ka), and the landscape just beyond the Fjord Stade moraines deglaciated ~10.2 ka. If the Jakobshavn Isbræ margin had experienced a more extensive late Holocene advance then it may have overran the Fjord Stade moraines and settled at a position abutting the 10.2 ka deglacial landscape. The magnitude of inland retreat during the middle Holocene (see Section 5.3 below) may have also influenced the deglaciation ages of the landscape just outboard of the historical moraine around the GrIS periphery. Extensive inland retreat during the middle Holocene followed by a small late Holocene readvance would result in the historical ice limit abutting a landscape with a relatively young deglaciation age compared to a separate ice-sheet sector that experienced minimal middle Holocene inland retreat and a similar late Holocene readvance.

The aforementioned factors almost certainly contributed to the asynchronous timing of deglaciation outboard of the historical moraine around the GrIS periphery, but in addition, regional differences in temperature change through the early to middle Holocene likely also contributed to Greenland's asynchronous deglaciation ages (e.g. Carlson et al., 2014). At Rink Isbræ, deglaciation of the landscape beyond the historical limit did not occur until sometime after 5.2 ka, yet deglaciation occurred ~3.5 kyr earlier ~150 km to the south at the Store Gletcher in the Ummannaq Trough system (Fig. 1), and almost 5 kyr earlier ~180 km to the north at Upernavik Isstrøm (Fig. 2). Although some regional climatic differences may have persisted between Upernavik Isstrøm, Rink Isbræ and Store Gletscher during the early to middle Holocene, it is unlikely that such a broad range in deglaciation ages across a relatively restricted geographical area can be fully attributed to climatic differences. Indeed, the local topography in the broader Ummannaq system likely contributed to the broad range in deglaciation ages where fjord narrowing and shallow bed depths acted as natural stabilization points that acted to interrupt outlet glacier retreat (Roberts et al., 2013; Lane et al., 2014). To thoroughly test the hypothesis that asynchronous timing of deglaciation primarily reflects differences in the timing of when temperatures first exceeded late Holocene temperatures, local to regional paleo-temperature records are needed that extend well before the timing of deglaciation. In any case, the pattern of deglaciation timing around Greenland is likely based on multiple factors.

5.2. Simulated pattern of final deglaciation compared to the geological record

Lecavalier et al. (2014) present the most recent simulated evolution of the GrIS through the Holocene using a three-dimension thermomechanical ice-sheet model originally published by Huybrechts and de Wolde (1999) and Huybrechts (2002; Fig. 2); Lecavalier et al.'s (2014) work is an update of that by Simpson et al. (2009). The efforts of Lecavalier et al. (2014) and Simpson et al. (2009) are particularly notable because they directly compare modeled patterns of sea-level change around the GrIS periphery driven by glacial isostatic adjustment, to geological reconstructions of relative sea level in order to assess model accuracy. In addition, their simulations explicitly use field observations constraining the lateral or vertical extent of the GrIS as boundary conditions (e.g. GrIS extent at the LGM). Lecavalier et al. (2014) model the evolution of the ice sheet from the LGM through present; however, here we discuss the modeled ice-margin outputs (henceforth referred to as Huy3) since ~12 ka because these results are most directly relevant for assessing 1) timing of landscape deglaciation just beyond the historical ice limit, and 2) the timing and magnitude of the minimum extent of the GrIS in the middle Holocene.

The Huy3 output places the entire GrIS margin on the continental shelf at 12 ka, with a noticeably more retracted ice margin at select cross-shelf troughs (Fig. 2). Off the West Greenland coast, the ice margin remained out on the continental shelf ~12.2 ka, consistent with the Huy3 output (Ó Cofaigh et al., 2013). In Southeast Greenland, the only comparable deglaciation ages are from the Torqulertivit Imiat valley located at the mouth of Sermilik Fjord (~12.7 ka) and at Kangerdlugssuaq Fjord (~11.8 ka; Fig. 2). The timing of deglaciation in the Torqulertivit Imiat valley has considerable uncertainty (12,660 ± 1200 yrs; Table 1), but this age is consistent with the 12 ka Huy3 margin resting near the valley mouth. Although the 12 ka Huy3 margin is situated east of the coast at Kangerdlugssuaq, the 12 ka limit is in general agreement with age of final deglaciation after considering the uncertainty in the Kangerdlugssuaq chronology (11,830 ± 1040 yrs; Table 1) and that the Huy3 output is able to capture the pattern of recessed ice margins in the Sermilik and Kangerdlugssuaq Fjord regions (i.e. earlier deglaciation) compared to the adjacent ice-sheet sectors that is consistent with the geological record (Fig. 2).

By 10 ka the Huy3 output depicts an ice sheet that is almost entirely land-based and the simulated 10 ka margin is generally consistent with deglaciation ages at Sermilik and Bernstorffs Fjord in Southeast Greenland. In Southwest Greenland, the simulated 10 ka margin is consistent with the timing of final deglaciation near Paamiut (10.7 ka), and also consistent with the deglacial chronology at Upernavik Isstrøm and the Melville Bugt region which reveals that the landscape outboard of the historical moraine deglaciated ~10 ka (Fig. 2). However, the Huy3 10 ka margin is too extensive at Narsarsuaq and the broader KNS region (Fig. 2) where ice had retreated behind its current position at 11.1 and 10.2–10.7 ka, respectively. The 9 ka Huy3 margin is similar to the 10 ka margin along much of the GrIS periphery, particularly in western and northwestern Greenland, although there is noticeable separation between the two limits between Disko Bugt and Kangerlussuaq. In the Disko Bugt and Ummannaq regions, the 9 ka limit is situated west of deglaciation ages that range from 8.7 ka at Store Gletscher to 7.5 ka at Jakobshavn Isfjord, and farther south in the KNS region, the Huy3 model continues to depict an ice margin that is too extensive compared to geological constraints. The 6 ka Huy3 margin is generally consistent with deglaciation ages that date to that time; final deglaciation in the Kangerlussuaq region occurred 7.0–6.8 ka compared to the 6 ka Huy3 limit that is situated inland of the current margin. Although the density of geological constraints

along northern Greenland is relatively sparse compared to other regions, existing constraints (all minimum ages) suggest that the GrIS was behind its present position ~7 ka. Yet, the 6 ka Huy3 margin is outboard of the historical limit.

Collectively, the Huy3 model predicts that the GrIS retreated behind its current margin between ~8 and 6 ka along West and Southwest Greenland, between ~10 and 9 ka in southern Greenland and >10 ka in the southeast, which is in reasonable agreement with geological records of deglaciation in these areas. The most obvious misfits between the Huy3 outputs and the geological record occur at 1) the broader KNS region where deglaciation occurred between 10.2 and 10.7 ka and the Huy3 model predicts deglaciation between ~6 and 4 ka, and 2) the Narsarsuaq region, where the margin retreated behind its current position at ~11.1 ka, compared to a Huy3 prediction of ~9 ka. Both the KNS and Narsarsuaq regions are dominated by marine-terminating outlet glaciers that are susceptible to dynamic processes that do not operate at land-terminating regions of the ice sheet. Indeed, dynamical processes and calving are not well represented in the Huy3 model. Instead the Huy3 model is built upon a shallow-ice approximation platform, which can reasonably simulate large-scale dynamics, but may perform poorly at the ice margin. Dynamical processes operating in the KNS and Narsarsuaq regions likely contributed to an earlier deglaciation in these areas compared to their adjacent margins, which may not be fully captured by the Huy3 output. Modeling efforts that are able to better resolve high velocity ice streams and outlet glaciers may improve model-data fits in regions where these features exist. Furthermore, incorporating an ocean temperature forcing component may also improve model-data misfits at marine-terminating margins of the GrIS as temperatures at the ice-ocean interface significantly influence ice-margin behavior (e.g. Rignot et al., 2010).

Another complexity that may contribute to the mismatch between geological constraints and the simulated evolution of the GrIS is the prescribed climate forcing within the Huy3 model. The Huy3 model is forced with the GRIP $\delta^{18}O$-derived temperature record (Dansgaard et al., 1993), which only reflects temperature at a single point in the interior of the ice sheet. In turn, the GRIP $\delta^{18}O$-derived temperature record is used to build a temperature profile across Greenland that forces the model. There were undoubtedly regionally varying temperature changes along the GrIS periphery during the early Holocene, which may help explain regional differences in the timing of deglaciation in addition to dynamical processes. While computationally taxing, future efforts should strive to incorporate a more realistic climate forcing that considers climate variability along the GrIS margin.

5.3. The minimum extent of the GrIS during the middle Holocene and subsequent late Holocene readvance

The most complete geological records that constrain the middle to late Holocene fluctuations of the GrIS are from Melville Bugt – Upernavik Isstrøm region, Jakobshavn Isfjord, Kangerlussuaq and the Narsarsuaq region.

5.3.1. Melville Bugt to Upernavik Isstrøm

At Melville Bugt deglaciation occurred ~9.5 ka (Fredskild, 1985; Bennike, 2008) before the ice margin retreated an unknown distance inland. However, numerous aspartic-acid inferred shell ages suggest that the minimum extent occurred ~5–3 ka. The ice margin likely approached its current position sometime during the LIA, but is unknown if the ice margin was near its current position at any time prior to the LIA. At Upernavik Isstrøm, ice retreated behind its current margin ~10.0 ka based on ^{10}Be ages and minimum-limiting radiocarbon ages from basal lake sediments (Briner et al., 2013), and numerous aspartic-acid inferred ages suggest that the ice margin here also achieved its minimum extent ~5–3 ka, although is unknown how far inland ice margin retreated (Briner et al., 2014). In addition, sediments from threshold lakes cored in the region indicate that Upernavik Isstrøm approached its current position by ~600 cal yr BP and perhaps as early as ~1070 cal yr BP, a few hundred years before the LIA (Briner et al., 2013).

5.3.2. Jakobshavn Isfjord

At Jakobshavn Isfjord, multiple records constrain the middle to late Holocene history of the ice margin (Fig. 3). Deglaciation of the landscape is robustly constrained to 7.5–7.6 ka (Fig. 2A), but following deglaciation, sediment records from Lake Lo (a threshold lake) just north of the Isfjord at Pâkitsoq indicate that the ice margin lingered near its present position until 5.4 cal ka BP before retreating at least 1.5 km inland of the present margin (Håkansson et al., 2014). This chronology is consistent with aspartic-acid inferred ages from reworked shells suggesting that the minimum extent was achieved sometime between ~5 and 3 ka at Jakobshavn Isfjord (Briner et al., 2014). In addition, sediments from Eqaluit Taserssuat (Fig. 3) suggest that following ice retreat out of the lake catchment, the ice margin readvanced and remained within the lake's catchment since 6–5 ka, although this record is poorly dated. Additional sediment records from nearby threshold lakes indicate that the ice-margin was similar to today as early as 2.3 cal ka BP, with the late Holocene maximum extent achieved ~400 cal yr BP (Figs. 3 and 6). Supporting this reconstruction are oceanographic records from the mouth of Jakobshavn Isfjord that suggest Jakobshavn Isbræ may have been relatively extensive between ~2.2 and 1.7 cal ka BP (Lloyd, 2006).

Considering that 1) the ice margin may have lingered near today's margin for an additional ~2 kyr following deglaciation of the landscape outboard of historical limit (Håkansson et al., 2014), 2) the GrIS has remained within Eqaluit Taserssuat catchment since ~6–5 ka, and 3) Jakobshavn Isbræ first approached its current position by ~2.3 cal ka BP, we suggest that the magnitude of middle Holocene retreat at Jakobshavn Isfjord was minimal. More extensive inland retreat would have been easier to achieve if the ice margin continued to race inland following deglaciation, but the Lake Lo record suggests that ice stagnated near its current margin following deglaciation. Greater inland retreat would also be supported if the threshold lake records all indicated that the ice margin did not reach its current position until sometime in the last few hundred years, but instead Jakobshavn Isbræ was near today's margin ~2.3 cal ka BP. Rather, it is unlikely that the ice sheet retreated several 10s of km inland by 5–3 ka and was then able to readvance and approach today's extent by ~2.3 cal ka BP. Weidick et al. (1990) suggested that the ice sheet in this region retreated 15–20 km inland during the middle Holocene. Based on the chronology presented here, we generally agree with this estimate, and further suggest that this may be a maximum limit on the distance of inland retreat during the middle Holocene. Furthermore, we note that the chronology of ice-margin change at Jakobshavn Isfjord appears to be closely linked to local summer temperature change (North Lake; Figs. 3 and 6). Jakobshavn Isbræ likely achieved its minimum extent ~5–3 ka, coinciding with the warmest temperatures in the North Lake record (2–3 °C above modern values), and a noticeable drop in temperatures occurs at ~3 ka, shortly before the ice margin first approached its current position ~2.3 cal ka BP. Jakobshavn Isbræ achieved its maximum late Holocene extent by ~400 cal ka BP, which coincides with the coolest temperatures recorded at North Lake over the last ~7 kyr.

5.3.3. Kangerlussuaq

Similar to Jakobshavn Isfjord, the Kangerlussuaq region benefits from robust constraints on the timing of deglaciation outboard of

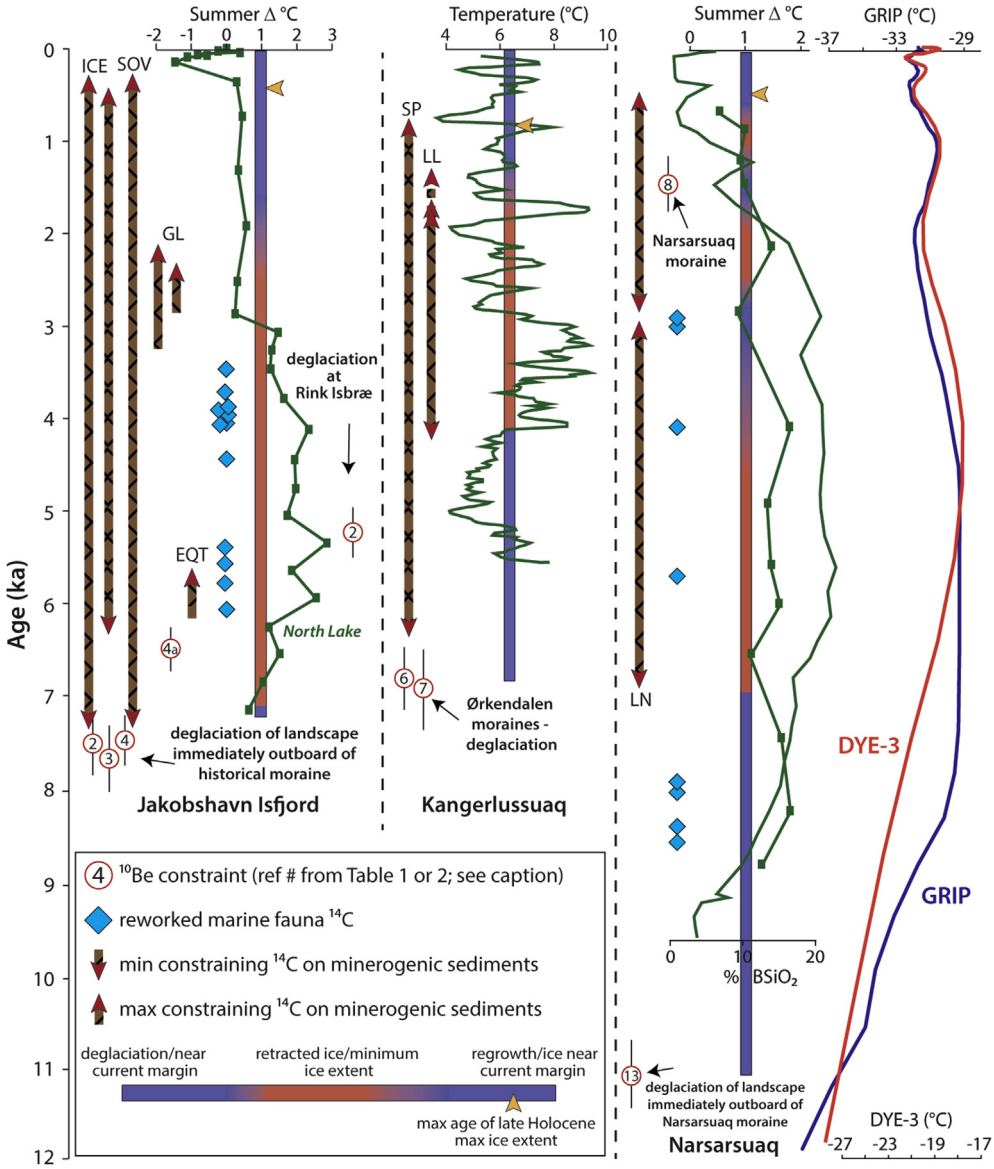

Fig. 6. Summary of the GrIS margin history at key sites in West and Southwest Greenland: Jakobshavn Isfjord, Kangerlussuaq and Narsarsuaq. Each section shows the timing of deglaciation, lake sediment records that constrain the timing and duration of a smaller-than-present ice sheet, and radiocarbon ages from shells reworked into the historical moraine. Blue and red shaded bar depict relative fluctuations of the ice margin at each location based on available geological records. At Jakobshavn Isfjord, the ice-margin chronology is compared to a local chironomid-based reconstruction of summer temperatures at North Lake (Fig. 3; Axford et al., 2013). At Kangerlussuaq, ice-margin fluctuations are compared to a local alkeone-based reconstruction of summer temperatures (D'Andrea et al., 2011). In the Narsarsuaq region, the record of ice-margin change is compared to a regional chironomid-based reconstruction of summer temperatures (Wooller et al., 2004; line with symbols) and a 9.5 kyr record of biogenic silica from nearby Qipisarqo (Kaplan et al., 2002; plain line). All records are compared to the GRIP and Dye-3 borehole temperature profiles (Dahl-Jensen et al., 1998). Note that the summer temperature record from North Lake at Jakobshavn Isfjord and the biogenic silica record from Qipisarqo generally mimic the GRIP and DYE-3 borehole temperature profiles. ICE-Ice Boom Lake, SOV-South Oval Lake, GL-Goose Lake, EQT-Eqaluit Taserssuat, SP-Sports Lake, LL-Lake Lucy, LN-Lower Nordbosø. Numbers in symbols are linked to Table 1 (#2-4a: Jakobshavn Isfjord and #6-7: Kangerlussuaq; #13: Narsarsuaq) and Table 2 (#2: Rink Isbræ and #8: Narsarsuaq).

the historical ice limit (van Tatenhove et al., 1996; Levy et al., 2012; Carlson et al., 2014), thus defining a clear interval when the ice sheet was smaller than today. Deglaciation occurred ~7.0–6.8 ka and the sediment record from Sports Lake confirms that between local deglaciation and the last millennium the ice margin was behind its current position. Based on the sediment record from nearby proglacial Lake Lucy, however, we suggest that following deglaciation 7.0–6.8 ka, the ice margin remained within ~900 m its current position until ~4.2 cal ka BP (Fig. 5). Between ~4.2 cal ka BP and ~1.8 cal BP the ice margin was >900 m inland of today, and since ~1.8 cal ka BP, the ice margin has generally remained within 900 m of its present position.

Another similarity between the Jakobshavn Isfjord and the Kangerlussuaq region is that following deglaciation the ice margin seemed to have lingered near its current position before retreating inland. Based on this interpretation at Kangerlussuaq, coupled with the fact that the ice margin was back out near its current position at ~1.8 ka, we suggest that the magnitude of GrIS retreat was minimal because there was only a ~2.4 kyr window of the time for the ice margin to retreat and then readvance. We consider it unlikely that this sector of the ice sheet retreated several 10s of km or up to ~120 km as suggested by model simulations during the middle Holocene (see Section 5.4 below; Tarasov and Peltier, 2003; Simpson et al., 2009). We cannot determine the exact distance of

inland retreat at the Kangerlussuaq margin, but we tentatively estimate retreat on the order of ~10 km during the middle Holocene based on the chronology presented here.

Furthermore, additional qualitative evidence provides supports our hypothesis that there was minimal ice-sheet retreat during the middle Holocene. This sector of the ice sheet is entirely land terminating and ice loss is only possible through surface melt making the rapid evacuation of ice and ice-margin retreat difficult. On the other hand, this sector of the GrIS retreated ~50 km per 1000 years between Sisimiut and the Kangerlussuaq region, indeed suggesting that a land-based margin can retreat a few tens of km in as little as 1000 years. However, surface melt rates may have been much higher between ~11 and 7 ka as Summit Greenland temperature records suggest this was the warmest part of the Holocene (Vinther et al., 2009). In this regard, perhaps most of the early to middle Holocene retreat had already taken place prior to 6.8 ka. By the time the ice margin retreated past the historical limit at 6.8 ka, it may have already been becoming cooler, and thus the ice margin may not have retreated much more inland after ~6.8 ka. In addition, the modern GrIS in the broader Kangerlussuaq region is generally within a few 10s of m or still resting directly on its historical moraine, whereas the ice margin at Jakobshavn Isfjord has retreated several kilometers behind its historical margin suggesting that the ice-sheet response to a similar climate forcing is vastly different between these two ice-sheet sectors. Indeed, Kelley et al. (2012) suggested that this land-terminating swath of the West GrIS is just beginning to, or has yet to respond to, contemporary warming because of long response times of this ice sheet sector to climate forcing. Collectively, these qualitative indicators support the notion that the Kangerlussuaq sector of the GrIS margin remained close to its current position through much of the Holocene.

Middle to late Holocene fluctuations of the Kangerlussuaq ice margin can also be compared to a regional alkenone-based record of summer temperature generated from lakes located ~50 km west of the ice margin (D'Andrea et al., 2011). This temperature record only spans the last ~5.6 kyr, but noticeable patterns emerge when comparing the reconstructed ice margin history to centennial-scale temperature trends (Fig. 6). The Lake Lucy record suggests that the ice margin was near its current margin until ~4.2 cal ka BP at which time the ice margin retreated behind Lake Lucy's topographic threshold. The timing of this transition is marked by a steep rise in regional temperatures recorded in the Kangerlussuaq temperature record (Fig. 6). The warmest reconstructed temperatures occur between ~3.2 and 3.0 cal ka BP, coinciding with a retracted ice margin between ~4.2 and 1.8 cal ka BP. Long-term cooling beginning ~3.0–2.8 cal ka BP culminated in a pronounced cold interval between 2.2 and 1.8 cal ka BP. The timing of this cold interval coincides with the reappearance of minerogenic sediments in the Lake Lucy record at ~1.8 cal ka BP, and thus an ice extent similar to today. Furthermore, Sports Lake sediments suggest that the ice-margin first attained a maximum late-Holocene position at 870 ± 65 cal yr BP. Although this is a maximum limiting age (see Section 4.2), it coincides with an abrupt temperature decline beginning ~850 cal yr BP seen in the Kangerlussuaq temperature record (Fig. 6). The Lake Lucy and Sports Lake records, combined with D'Andrea et al. (2011) temperature record indicate that, much like the ice-margin at Jakobshavn Isfjord, ice-margin fluctuations at Kangerlussuaq are tightly coupled to local temperatures. However, key for further deciphering the Holocene history of the ice margin will be to develop a robust local temperature reconstruction that spans the full regional deglaciation history. Did the extensive retreat of the ice margin between ~10 and 7 ka (Sisimiut to Kangerlussuaq) coincide with the warmest regional temperatures of the Holocene, or does the interval of warmer temperatures between ~4.1 and 2.8 cal ka BP reconstructed by D'Andrea et al. (2011) that coincide with the minimum extent of the GrIS, represent this region's Holocene thermal maximum?

5.3.4. Narsarsuaq

The Holocene history of the GrIS in the Narsarsuaq region is constrained by precise deglaciation ages from outboard of the historical ice limit and sediments from Lower Nordbosø (Fig. 6). Although regional deglaciation occurred 11.1 ka (Carlson et al., 2014), sediments from Lower Nordbosø reveal that the ice margin likely remained relatively close to the historical maximum until 6.9 ka (Larsen et al., 2011). A retracted ice extent beginning 6.9 ka was interrupted by a readvance of the ice sheet culminating ~3.0–2.8 cal ka BP, followed by a second period of a retracted ice margin, and finally an ice extent similar to present since ~0.5 cal ka BP. Similar to the records at Jakobshavn Isfjord and Kangerlussuaq, the most striking feature of this chronology is that the ice margin lingered near the ice limit for ~4 kyr after initial deglaciation. The ice margin achieved its minimum extent sometime after but 6.9 ka, but the ice margin was back near its current position by 3.0–2.8 ka leaving only 4 kyr for the ice sheet to complete its advance and retreat cycle. Moreover, at least one sector achieved its late Holocene maximum prior to the LIA as the Narsarsuaq moraines are dated to be slightly older than 1.5 ka (Bennike and Sparrenbom, 2007; Winsor et al., 2014). It is somewhat surprising that this sector of the ice sheet obtained its late Holocene maximum extent ~1.2–1.5 ka, and that this ice limit was so far beyond the historical moraine because moraines dating to this age, regardless of distance beyond the historical moraine, have yet to be found anywhere else in Greenland. On the other hand, the Narsarsuaq moraines could reflect a unique local to regional climate in southern Greenland. Indeed, Andresen et al. (2004) and Seidenkrantz et al. (2007) note cooler conditions just prior to ~1.5 ka in southern Greenland based on a variety of proxies. In any case, the overall Narsarsuaq geological record hints at muted inland retreat during the middle Holocene.

5.4. Simulated middle Holocene minimum GrIS extent compared to the geological record: a relatively stable GrIS margin through the middle Holocene?

Around much of the GrIS periphery, the simulated 9–4 ka margins are relatively similar and are all situated near the current GrIS margin making it difficult to assess their accuracy when compared to the geological record. However, geological evidence from along West and Southwest Greenland make it clear that the GrIS was smaller-than-today during the middle Holocene and then expanded over the last few thousand years before reaching its late Holocene maximum. In the broader Kangerlussuaq region in Southwest Greenland, model simulations depict large-scale retreat ranging from ~20 to 60 km inland at 4 ka (Lecavalier et al., 2014) to >100 km at 8 ka (Fig. 2; Tarasov and Peltier, 2003). The Huy3 output predicts that deglaciation of the Kangerlussuaq region occurred ~8–6 ka, consistent with the geological record, but from here the records diverge. Our geological reconstruction suggests that ice remained close to the present margin until ~4.2 cal ka BP, whereas the Huy3 model simulates a GrIS margin that achieved its minimum extent at 4 ka. Considering that the Kangerlussuaq margin was near its current margin until ~4.2 cal ka BP and readvanced to approach its current margin by ~1.8 cal ka BP, we suggest a more likely timing for the GrIS minimum in this region is closer to ~3 ka and the ice margin retreated on the order of <10 km rather than several 10s of km. Moreover, when our geological reconstruction in the Kangerlussuaq region is combined with ice-margin histories from Jakobshavn Isfjord and the Narsarsuaq region, it further suggests that in contrast to model simulations, the magnitude of inland

retreat during the middle Holocene was rather limited. The modeled minimum ice sheet in Lecavalier et al. (2014) at 4 ka equates to a 0.16 m sea-level contribution, but considering minimal inland retreat of the ice margin based on geological reconstructions, we suggest that this value may be a maximum estimate of the GrIS contribution to sea level in the middle Holocene. Although we speculate that the Huy3 minimum ice-sheet configuration may overestimate the magnitude of GrIS mass loss during the middle Holocene, the Huy3 simulation does depict a slightly larger ice sheet at 4 ka with less inland retreat in the Kangerlussuaq region than Simpson et al. (2009) who simulate a minimum ice sheet that equates to a 0.17 m sea-level contribution. Nonetheless, regardless of the exact distance of inland retreat, a smaller-than-present ice sheet and subsequent regrowth is supported by relative sea-level data from the Sisimiut region west of Kangerlussuaq indicate there was a sea-level rise of 5 m over the last 2–3 ka interpreted to represent a readvance of the GrIS (Long et al., 2011).

One possible reason that the Huy3 model may over predict the magnitude of middle Holocene retreat is the prescribed model temperature forcing. As mentioned in Section 5.2, the sole temperature forcing is based on the GRIP $\delta^{18}O$ record, which is used to build a temperature profile across Greenland. Following Simpson et al. (2009) and Lecavalier et al. (2014) had to impose a Holocene thermal maximum onto the GRIP $\delta^{18}O$ profile in order to trigger inland retreat of the ice margin. However, Lecavalier et al. (2014) allowed the magnitude of this imposed thermal maximum to change in order to achieve a better model-data fit. Whereas this process resulted in simulations that were more consistent with isolation-basin-derived relative seal-level data, it may have resulted in over estimating the amount of marginal inland retreat. On the other hand, intervals of warmer than present temperatures are indeed depicted in the GRIP and Dye-3 borehole temperature profiles and in temperature reconstructions along the West and Southwest GrIS periphery (Fig. 6; D'Andrea et al., 2011; Axford et al., 2013). Perhaps simulations that can successfully incorporate climate reconstructions developed at the ice-sheet margin when generating an ice-sheet wide temperature profile will provide better model-data fits.

It is also worth noting that the Huy3 model has a resolution of 20 × 20 km, which almost certainly contributes to model-data mismatches. The ice margin in the Kangerlussuaq region has a relatively low profile and relatively modest changes in the regional snowline may result in large fluctuations in the lateral position of the ice margin. Rather, snowline fluctuations result in the simulated Huy3 ice margin advancing or retreating in 20 km cells and an overestimate in snowline rise could magnify the magnitude of inland retreat if the margin is forced to evolve at 20 km increments. New modeling efforts at higher spatial resolution may improve the fit between modeled and reconstructed ice margins, however this will become computationally expensive.

The geological record reviewed here and the model results of Simpson et al. (2009) and Lecavalier et al. (2014), although differing slightly, all point to minimal inland retreat of the West and Southwest GrIS through the Holocene despite warmer-than-present temperatures; increased accumulation over the ice-sheet interior is the most obvious mechanism that may explain this relative Holocene stability. Although temperature records from the ice-sheet interior and around the West GrIS periphery all depict warmer-than-present temperatures through the middle Holocene (i.e. Holocene Thermal Maximum), accumulation records from summit Greenland indicate that there was a ~200% percent increase in accumulation over the ice sheet between ~12 ka and today (Cuffey and Clow, 1997). Temperature is the primary driver of overall glacier and ice-sheet mass balance, but a ~200% increase in precipitation must have, to some degree, influenced the evolution of the GrIS through the Holocene by counteracting the effects of warmer-than-present temperatures on GrIS mass balance. In addition to increasing the number of temperature reconstructions along the GrIS periphery that are incorporated into ice-sheet simulations, reconstructions of paleo-precipitation through the Holocene are needed in order to fully assess the role of precipitation in driving Holocene ice-sheet change.

6. Conclusions

There has been significant progress in the last 5+ years in developing robust deglaciation chronologies around the GrIS periphery and a key outcome of this work are the precise constraints on the timing of when in the early Holocene the GrIS margin retreated behind its late Holocene maximum extent. In addition, new records are emerging that are able to better elucidate the history of the GrIS margin when it was smaller than today, and in some regions complete records spanning late-glacial and early Holocene deglaciation to late Holocene expansion of the GrIS are now in place. Collectively, these records are well-suited for assessing the accuracy of geophysical ice-sheet model simulations. The compilation of geological records and available model simulations considered here reveals:

- The timing of when the GrIS margin retreated behind the late Holocene maximum extent constrained by the geological record is duplicated quite well by the available model simulations, although notable discrepancies exist in Southwest Greenland in the broader Nuuk and Narsarsuaq regions where simulated deglaciation occurs too late compared to the geological record.
- In Southwest Greenland, model simulations likely overestimate the magnitude of ice-sheet retreat in the middle Holocene.
- Key considerations for ice-sheet modeling that may improve model-data misfits include the better representation of 1) ice-dynamical process, including better resolved ice streams and marine-terminating outlet glaciers, 2) an ocean temperature forcing component, 3) more realistic climate input parameters that consider climate reconstructions from the ice-sheet margins, both temperature and precipitation, and 4) higher spatial resolution.
- Although firm constraints on the timing and magnitude of ice sheet retreat during the middle Holocene are limited, reconstructions from Jakobshavn Isfjord, the Kangerlussuaq region and Narsarsuaq all suggest minimal ice recession during the middle Holocene. These records hint at a relatively stable ice-margin through the middle Holocene, but more records are needed to confirm this hypothesis. The GrIS likely achieved its minimum extent between ~5 and 3 ka, although the timing of the minimum ice extent from region to region is likely asynchronous.
- In general, the timing of the minimum GrIS ice extent post-dates the timing of peak borehole temperatures from Summit Greenland (Fig. 6) and the timing of retracted ice from other glacierized areas in the broader Baffin Bay–Greenland region. Recent records from Baffin Island suggest that following a minimum ice extent, glacier and ice caps were expanding again by ~5 ka (Miller et al., 2013), and in Iceland, glacier expansion may have begun as early as ~6 ka (Geirsdóttir et al., 2009). However, these records focus on alpine glaciers whose oscillations are more likely to be in-sync with centennial-scale regional climate variations compared to oscillations of the GrIS margin.
- Sediment records from threshold lakes combined with high-resolution maps of sub-ice topography is a powerful new approach for elucidating the history of a smaller-than-present

GrIS. To the best of our knowledge, this method currently provides the only way to directly establish absolute constraints on the magnitude of inland retreat. More records combining these two approaches are needed.

- A close link between reconstructed ice-margin fluctuations and records of local to regional temperature change is observed at least at two locations in West Greenland (Jakobshavn Isfjord and Kangerlussuaq).
- Lake records and at least one moraine complex (Narsarsuaq moraines) indicate that there were several time periods when the ice margin approached its late Holocene maximum prior to the LIA.

Acknowledgments

NEY acknowledges support from a Lamont-Doherty Post-doctoral Fellowship, an award from the Lamont Climate Center and NSF-BCS award #1002597. JPB acknowledges support from NSF-BCS awards #752848 and #1156361. We thank Mathieu Morlighem for providing sub-ice elevation data and Joerg Schaefer for numerous insightful discussions during the preparation of this manuscript. We also thank Yarrow Axford, Sandra Cronauer, Chris Kuzawa and Sam Kelley for help coring Lake Lucy and Sports Lake. Finally, we thank Anders Schomacker and an anonymous reviewer for comments that helped improve this manuscript. This is LDEO contribution #7868.

Appendix A. Supplementary data

Supplementary data related to this article can be found at http://dx.doi.org/10.1016/j.quascirev.2015.01.018.

References

Andresen, C.S., Björck, S., Bennike, O., Bond, G., 2004. Holocene climate changes in southern Greenland: evidence from lake sediments. J. Quat. Sci. 18, 783–795.
Axford, Y.A., Losee, S., Briner, J.P., Francis, D.R., Langdon, P.G., Walker, I.R., 2013. Holocene temperature history at the western Greenland Ice Sheet margin reconstructed from lake sediments. Quat. Sci. Rev. 59, 87–100. http://dx.doi.org/10.1016/j.quascirev.2012.10.024.
Balco, G., Stone, J.O., Lifton, N.A., Dunai, T.J., 2008. A complete and easily accessible means of calculating surface exposure ages or erosion rates from ^{10}Be and ^{26}Al measurements. Quat. Geochronol. 33, 174–195. http://dx.doi.org/10.1016/j.quageo.2007.12.001.
Balco, G., Briner, J.P., Finkel, R.C., Rayburn, J.A., Ridge, J.C., Schaefer, J.M., 2009. Regional beryllium-10 production rate calibration for late-glacial northeastern North America. Quat. Geochronol. 4, 93–107.
Bamber, J.L., et al., 2013. A new bed elevation dataset for Greenland. Cryosphere 7, 499–510. http://dx.doi.org/10.5194/tc-7-499-2013.
Bennike, O., 2000. Palaeoecological studies of Holocene lake sediments from west Greenland. Palaeogeogr. Palaeoclimatol. Palaeoecol. 155, 285–304.
Bennike, O., 2002. Late Quaternary history of Washington Land, North Greenland. Boreas 31, 260–272.
Bennike, O., 2008. An early Holocene Greenland whale from Melville Bugt, Greenland. Quat. Res. 69, 72–76. http://dx.doi.org/10.1016/j.yqres. 2007. 10.004.
Bennike, O., Weidick, A., 2001. Late Quaternary history around Nioghalvfjerdsfjorden and Jøkelbugten, North-East Greenland. Boreas 30, 205–227.
Bennike, O., Björck, S., 2002. Chronology of the last recession of the Greenland Ice Sheet. J. Quat. Sci. 17, 211–219. http://dx.doi.org/10.1002/jqs.670.
Bennike, O., Sparrenbom, C.J., 2007. Dating of the Narsarssuaq stade in southern Greenland. Holocene 17, 279–282.
Bennike, O., Wagner, B., Richter, A., 2011. Relative sea level changes during the Holocene in the Sisimiut area, south-western Greenland. J. Quat. Sci. 26, 353–361. http://dx.doi.org/10.1002/jqs.1458.
Bindschadler, R.A., et al., 2013. Ice-sheet model sensitivities to environmental forcing and their use in projecting future sea level (the SeaRISE project). J. Glaciol. 59, 195–224. http://dx.doi.org/10.3189/2013JoG12J125.
Briner, J.P., Kaufman, D.S., Bennike, O., Kosnik, M.A., 2014. Amino acid ratios in reworked marine bivalve shells constrain Greenland Ice Sheet history during the Holocene. Geology 42, 75–78. http://dx.doi.org/10.1130/G34843.1.
Briner, J.P., Håkansson, L., Bennike, O., 2013. The deglaciation and neoglaciation of Upernavik Isstrøm, Greenland. Quat. Res. 80, 459–467. http://dx.doi.org/10.1016/j.yqres.2013.09.008.
Briner, J.P., Stewart, H.A.M., Young, N.E., Philipps, W., Losee, S., 2010. Using proglacial-threshold lakes to constrain fluctuations of the Jakobshavn Isbræ ice margin, western Greenland, during the Holocene. Quat. Sci. Rev. 29, 3861–3874. http://dx.doi.org/10.1016/j.quascirev.2010.09.005.
Carlson, A.E., Stoner, J.S., Donnelly, J.P., Hillaire-Marcel, C., 2008. Response of the southern Greenland Ice Sheet during the last two deglaciations. Geology 36, 359. http://dx.doi.org/10.1130/G24519A.1.
Carlson, A.E., Winsor, K., Ullman, D.J., Brook, E.J., Rood, D.H., Axford, Y., LeGrande, A.N., Anslow, F.S., Sinclair, G., 2014. Earliest Holocene south Greenland ice sheet retreat within its late Holocene extent. Geophys. Res. Lett. 41, 1–8. http://dx.doi.org/10.1002/(ISSN)1944-8007.
Church, J.A., et al., 2013. Sea level change. In: Stocker, T.F., Qin, D., Plattner, G.-K., Tignor, M., Allen, S.K., Boschung, J., Nauels, A., Xia, Y., Bex, V., Midgley, P.M. (Eds.), Climate Change 2013: the Physical Science Basis. Contribution of Working Group I to the Fifth Assessment Report of the Intergovernmental Panel on Climate Change. Cambridge University Press, Cambridge, United Kingdom and New York, NY, USA.
Collins, M., et al., 2013. Long-term climate change: projections, commitments and irreversibility. In: Stocker, T.F., Qin, D., Plattner, G.-K., Tignor, M., Allen, S.K., Boschung, J., Nauels, A., Xia, Y., Bex, V., Midgley, P.M. (Eds.), Climate Change 2013: the Physical Science Basis. Contribution of Working Group I to the Fifth Assessment Report of the Intergovernmental Panel on Climate Change. Cambridge University Press, Cambridge, United Kingdom and New York, NY, USA.
Colville, E.J., Carlson, A.E., Beard, B.L., Hatfield, R.G., Stoner, J.S., Reyes, A.V., Ullman, D.J., 2011. Sr-Nd-Pb Isotope evidence for Ice-Sheet presence on Southern Greenland during the Last Interglacial. Science 333, 620–623. http://dx.doi.org/10.1126/science.1204531.
Corbett, L.B., Bierman, P.R., Everett Lasher, G., Rood, D.H., 2015. Landscape chronology and glacial history in Thule, northwest Greenland. Quat. Sci. Rev. 109, 57–67. http://dx.doi.org/10.1016/j.quascirev.2014.11.019.
Corbett, L.B., Bierman, P.R., Graly, J.A., Neumann, T.A., Rood, D.H., 2013. Constraining landscape history and glacial erosivity using paired cosmogenic nuclides in Upernavik, northwest Greenland. Geol. Soc. Am. Bull. 125, 1539–1553. http://dx.doi.org/10.1130/B30813.1.
Corbett, L.B., Young, N.E., Bierman, P.R., Briner, J.P., Neumann, T.A., Rood, D.H., Graly, J.A., 2011. Paired bedrock and boulder ^{10}Be concentrations resulting from early Holocene ice retreat near Jakobshavn Isfjord, western Greenland. Quat. Sci. Rev. 30, 1739–1749. http://dx.doi.org/10.1016/j.quascirev.2011.04.001.
Cuffey, K.M., Clow, G.D., 1997. Temperature, accumulation, and ice sheet elevation in central Greenland through the last deglacial transition. J. Geophys. Res. 102, 26,383–26,396.
D'Andrea, W.J., Huang, Y., Fritz, S.C., Anderson, N.J., 2011. Abrupt Holocene climate change as an important factor for human migration in West Greenland. PNAS 108, 9765–9769.
Dahl-Jensen, D., Mosegaard, K., Gundestrup, N., Clow, G.D., Johnsen, S.J., Hansen, A.W., Balling, N., 1998. Past temperature directly from the Greenland Ice Sheet. Science 282, 268–271.
Dansgaard, W., et al., 1993. Evidence for general instability of past climate from a 250-kyr ice-core record. Nature 364, 218–220.
Dyke, L.M., Hughes, A.L.C., Murray, T., Hiemstra, J.F., Andresen, C.S., Rodés, A., 2014. Evidence for the asynchronous retreat of large outlet glaciers in southeast Greenland at the end of the last glaciation. Quat. Sci. Rev. 99, 244–259. http://dx.doi.org/10.1016/j.quascirev.2014.06.001.
Forman, S.L., Marín, L., van der Veen, C., Tremper, C., Csatho, B., 2007. Little Ice Age and neoglacial landforms at the Inland Ice margin, Isunguata Sermia, Kangerlussuaq, west Greenland. Boreas 36, 341–351.
Fredskild, B., 1985. The Holocene vegetational development of Tugtuligssuaq and Qeqertat, Northwest Greenland. Meddelelser om Grønland. Geoscience 14, 20 pp.
Funder, S., 1978. Holocene stratigraphy and vegetation history in the Scoresby Sund area, East Greenland. Bull. Grønl. Geol. Unders. 129, 66.
Funder, S., 1982. Rapport Grønlands Geologiske Undersøgelse. ^{14}C-dating of samples collected during the 1979 expedition to North Greenland, vol. 110, pp. 9–14.
Funder, S., Kjeldsen, K.K., Kjær, K.H., Ó Cofaigh, C., 2011. The Greenland Ice Sheet during the past 300,000 years: a review. Quat. Glaciat. Extent Chronol. 15, 699–713. http://dx.doi.org/10.1016/B978-0-444-53447-7.00050-7.
Geirsdóttir, A., Miller, G.H., Axford, Y., Ólafsdóttir, S., 2009. Holocene and latest Pleistocene climate and glacier fluctuations in Iceland. Quat. Sci. Rev. 28, 2107–2118.
Håkansson, S., 1976. University of Lund radiocarbon dates IX. Radiocarbon 18, 290–320.
Håkansson, L., Briner, J., Andresen, C.S., Thomas, E.K., Bennike, O., 2014. Slow retreat of a land based sector of the West Greenland Ice Sheet during the Holocene Thermal Maximum: evidence from threshold lakes at Paakitsoq. Quat. Sci. Rev. 98, 74–83.
Hjort, C., 1981. A glacial chronology for northern East Greenland. Boreas 10, 259–274.
Holland, D.M., Thomas, R.H., de Young, B., Ribergaard, M.H., Lyberth, B., 2008. Acceleration of Jakobshavn Isbræ triggered by warm subsurface ocean waters. Nat. Geosci. 1, 659–664. http://dx.doi.org/10.1038/ngeo316.
Hughes, A.L.C., Rainsley, E., Murray, T., Fogwill, C.J., Schnabel, C., Xu, S., 2012. Rapid response of Helheim Glacier, southeast Greenland, to early Holocene climate warming. Geology 40, 427–430. http://dx.doi.org/10.1130/G32730.1.

Huybrechts, P., 2002. Sea-level changes at the LGM from ice-dynamic reconstructions of the Greenland and Antarctic ice sheets during the glacial cycles. Quat. Sci. Rev. 21, 203–231.
Huybrechts, P., de Wolde, J., 1999. The dynamic response of the Greenland and Antarctic ice sheets to multiple-century climatic warming. J. Clim. 12, 2169–2188.
Kaplan, M., Wolfe, A.P., Miller, G.H., 2002. Holocene environmental variability in Southern Greenland inferred from Lake sediments. Quat. Res. 58, 149–159. http://dx.doi.org/10.1006/qres.2002.2352.
Kaufman, D., et al., 2004. Holocene thermal maximum in the western Arctic (0–180°W). Quat. Sci. Rev. 23, 529–560. http://dx.doi.org/10.1016/j.quascirev.2003.09.007.
Kelley, S.E., Briner, J.P., Young, N.E., Babonis, G.S., Csatho, B., 2012. Maximum late Holocene extent of the western Greenland Ice Sheet during the late 20th century. Quat. Sci. Rev. 56, 89–98. http://dx.doi.org/10.1016/j.quascirev.2012.09.016.
Kelley, S.E., Briner, J.P., Young, N.E., 2013. Rapid ice retreat in Disko Bugt supported by ^{10}Be dating of the last recession of the western Greenland Ice Sheet. Quat. Sci. Rev. 82, 13–22.
Kelly, M., Bennike, O., 1992. Rapport Grønlands Geologiske Undersøgelse, 34 pp. Quaternary Geology of Western and Central North Greenland, vol. 153.
Landvik, J.Y., Weidick, A., Hansen, A., 2001. The glacial history of the Hans Tausen Iskappe and the last glaciation of Peary Land, North Greenland. Meddelelser om Grønl. Geosci. 39, 27–44.
Lane, T.P., Roberts, D.H., Rea, B.R., Cofaigh, C.Ó., Vieli, A., Rodés, A., 2014. Controls upon the Last Glacial Maximum deglaciation of the northern Uummannaq Ice Stream System, West Greenland. Quat. Sci. Rev. 92, 324–344. http://dx.doi.org/10.1016/j.quascirev.2013.09.013.
Larsen, N.K., Kjær, K.H., Olsen, J., Funder, S., Kjeldsen, K.K., Nørgaard-Pedersen, N., 2011. Restricted impact of Holocene climate variations on the southern Greenland Ice Sheet. Quat. Sci. Rev. 30, 3171–3180. http://dx.doi.org/10.1016/j.quascirev.2011.07.022.
Larsen, N.K., Funder, S., Kjær, K.H., Kjeldsen, K.K., Knudsen, M.F., Linge, H., 2014. Rapid early Holocene ice retreat in West Greenland. Quat. Sci. Rev. 92, 310–323. http://dx.doi.org/10.1016/j.quascirev.2013.05.027.
Lecavalier, B.S., et al., 2014. A model of Greenland ice sheet deglaciation constrained by observations of relative sea level and ice extent. Quat. Sci. Rev. 102, 54–84. http://dx.doi.org/10.1016/jquascirev.2014.07.018.
Levy, L., Kelly, M.A., Howley, J.A., Virginia, R.A., 2012. Age of the Orkendalen moraines, Kangerlussuaq, Greenland: constraints on the extent of the southwestern margin of the Greenland Ice Sheet during the Holocene. Quat. Sci. Rev. 52, 1–5. http://dx.doi.org/10.1016/j.quascirev.2012.07.021.
Lloyd, J., 2006. Late Holocene environmental change in Disko Bugt, west Greenland: interaction between climate, ocean circulation and Jakobshavn Isbrae. Boreas 35, 35–49.
Long, A.J., Roberts, D.H., Dawson, S., 2006. Early Holocene history of the west Greenland Ice Sheet and the GH-8.2 event. Quat. Sci. Rev. 25, 904–922.
Long, A.J., Woodroffe, S.A., Roberts, D.H., Dawson, S., 2011. Isolation basins, sea-level changes and the Holocene history of the Greenland Ice Sheet. Quat. Sci. Rev. 1–21. http://dx.doi.org/10.1016/j.quascirev.2011.10.013.
Masson-Delmotte, V., et al., 2013. Information from paleoclimate archives. In: Stocker, T.F., Qin, D., Plattner, G.-K., Tignor, M., Allen, S.K., Boschung, J., Nauels, A., Xia, Y., Bex, V., Midgley, P.M. (Eds.), Climate Change 2013: the Physical Science Basis. Contribution of Working Group I to the Fifth Assessment Report of the Intergovernmental Panel on Climate Change. Cambridge University Press, Cambridge, United Kingdom and New York, NY, USA.
Miller, G.H., Alley, R.B., Brigham-Grette, J., Fitzpatrick, J.J., Polyak, L., Serreze, M.C., White, J.W.C., 2010a. Arctic amplification: can the past constrain the future? Quat. Sci. Rev. 29, 1779–1790. http://dx.doi.org/10.1016/j.quascirev.2010.02.008.
Miller, G.H., et al., 2010b. Temperature and precipitation history of the Arctic. Quat. Sci. Rev. 29, 1679–1715. http://dx.doi.org/10.1016/j.quascirev.2010.03.001.
Miller, G.H., Leham, S.J., Refsnider, K.A., Southon, J.R., Zhong, Y., 2013. Unprecedented recent summer warmth in Arctic Canada. Geophys. Res. Lett. 40, 1–7. http://dx.doi.org/10.1002/2013GL057188.
Morlighem, M., Rignot, E., Mouginot, J., Wu, X., Seroussi, H., Laroue, E., Paden, J., 2013. High-resolution bed topography mapping of Russell Glacier, Greenland, inferred from operation Ice Bridge data. J. Glaciol. 59, 1015–1023.
Morlighem, M., Rignot, E., Mouginot, J., Seroussi, H., Larour, E., 2014. Deeply incised submarine glacial valleys beneath the Greenland ice sheet. Nat. Geosci. 7, 418–422.
NEEM Community Members, 2013. Eemian interglacial reconstructed from a Greenland folded ice core. Nature 493, 489–494.
Nørgaard-Pedersen, N., Mikkelsen, N., 2009. 8000 year marine record of climate variability and fjord dynamics from Southern Greenland. Mar. Geol. 264, 177–189.
Nowicki, S., et al., 2013. Insights into spatial sensitivities of ice mass response to environmental change from the SeaRISE ice sheet modeling project II: Greenland. J. Geophys. Res. 118, 1025–1044. http://dx.doi.org/10.1002/jgrf.20076.
Ó Cofaigh, C., et al., 2013. An extensive and dynamic ice sheet on the West Greenland shelf during the Last Glacial cycle. Geology 41, 219–222.
Otto-Bliesner, B.L., Marshall, S.J., Overpeck, J.T., Miller, G.H., Hu, A., CAPE Project Members, 2006. Simulating Arctic climate warmth and icefield retreat in the Last Interglaciation. Science 311, 1751–1753. http://dx.doi.org/10.1126/science.1120808.
Reimer, P.J., et al., 2009. IntCal09 and Marine09 radiocarbon age calibration. Radiocarbon 51, 1111–1150.
Reyes, A.V., Carlson, A.E., Beard, B.L., Hatfield, R.G., Stoner, J.S., Winsor, K., Welke, B., Ullman, D.J., 2014. South Greenland ice-sheet collapse during Marine Isotope Stage 11. Nature 510, 525–528.
Rignot, E., Koppes, M., Velicogna, I., 2010. Rapid submarine melting of the calving faces of West Greenland glaciers. Nat. Geosci. 3, 187–191. http://dx.doi.org/10.1038/ngeo765.
Roberts, D.H., Long, A.J., Schnabel, C., Freeman, S., Simpson, M.J.R., 2008. The deglacial history of southeast sector of the Greenland Ice Sheet during the Last Glacial Maximum. Quat. Sci. Rev. 27, 1505–1516. http://dx.doi.org/10.1016/j.quascirev.2008.04.008.
Roberts, D.H., Rea, B.R., Lane, T.P., Schnabel, C., Rodés, A., 2013. New constraints on Greenland ice sheet dynamics during the Last Glacial cycle: evidence from the Uummannaq ice stream system. J. Geophys. Res. Earth Surf. 118, 519–541. http://dx.doi.org/10.1002/jgrf.20032.
Seidenkrantz, M.-S., Aagaard-Sørensen, S., Sulsbrück, H., Kuijpers, A., Jensen, K.G., Kunzendorf, H., 2007. Hydrography and climate of the last 4400 years in a SW Greenland fjord: implications for Labrador Sea palaeoceanography. Holocene 17, 387–401.
Simpson, M.J.R., Milne, G.A., Huybrechts, P., Long, A.J., 2009. Calibrating a glaciological model of the Greenland ice sheet from the Last Glacial Maximum to present-day using field observations of relative sea level and ice extent. Quat. Sci. Rev. 28, 1631–1657.
Sparrenbom, C.J., 2006. Constraining the Southern Part of the Greenland Ice Sheet Since the Last Glacial Maximum from Relative Sea-level Changes, Cosmogenic Dates and Glacio-isostatic Adjustment Models. PhD thesis. Lund University. LUNQUA Thesis 56.
Stuiver, M., Reimer, P.J., Reimer, R.W., 2005. CALIB 7.0. http://calib.qub.ac.uk/calib/.
Tarasov, L., Peltier, W.R., 2003. Greenland glacial history, borehole constraints, and Eemian extent. J. Geophys. Res. 108, 2143.
Ten Brink, N.W., 1975. Holocene history of the Greenland Ice Sheet based on radiocarbon-dated moraines in west Greenland. Meddelelser om Grønl. 44, 113 pp.
Ten Brink, N., Weidick, A., 1974. Greenland Ice Sheet history since the last glaciation. Quat. Res. 4, 429–440.
van de Berg, W.J., van den Broeke, M., Ettema, J., van Meijgaard, E., Kaspar, F., 2011. Significant contribution of insolation to Eemian melting of the Greenland ice sheet. Nat. Geosci. 4, 1–5. http://dx.doi.org/10.1038/ngeo1245.
van Tatenhove, F.G., van der Meer, J.J., Koster, E.A., 1996. Implications for deglaciation chronology from new AMS age determinations in central West Greenland. Quat. Res. 45, 245–253.
Vinther, B., Buchardt, S., Clausen, H., Dahl-Jensen, D., Johnsen, S., Fisher, D., Koerner, R., Raynaud, D., Lipenkov, V., Andersen, K., 2009. Holocene thinning of the Greenland ice sheet. Nature 461, 385–388.
Weidick, A., 1968. Observations on some Holocene glacier fluctuations in West Greenland. Meddelelser om Grønl. 165, 202.
Weidick, A., 1976. Glaciation and the Quaternary of Greenland. Grønl. Geol. Unders. 431–458.
Weidick, A., 1977. Rapport Grønlands Geologiske Undersøgelse. ^{14}C dating of survey material carried out in 1976, vol. 85, pp. 127–129.
Weidick, A., 1978. Rapport Grønlands Geologiske Undersøgelse. ^{14}C dating of survey material carried out in 1977, vol. 90, pp. 119–124.
Weidick, A., Bennike, O., 2007. Quaternary glaciation history and glaciology of Jakobshavn Isbræ and the Disko Bugt region, West Greenland: a review. Geol. Surv. Den. Greenl. 14, 78 p.
Weidick, A., Bennike, O., Citterio, M., Norgaard-Pedersen, N., 2012. Neoglacial and historical glacier changes around Kangersuneq fjord in southern West Greenland. Geol. Surv. Den. Greenl. 27, 1–68.
Weidick, A., Oerter, H., Reeh, N., Thomsen, H.H., Thorning, L., 1990. The recession of the Inland Ice margin during the Holocene climatic optimum in the Jakobshavn-Isfjord area of West Greenland. Glob. Planet. Change 82, 389–399.
Willemse, N.W., Koster, E.A., Hoogakker, B., van Tatenhove, F.G.M., 2003. A continuous record of Holocene eolian activity in West Greenland. Quat. Res. 59, 322–334.
Winsor, K., Carlson, A.E., Rood, D.H., 2014. ^{10}Be dating of the Narsarsuaq moraine in southernmost Greenland: evidence for a late-Holocene ice advance exceeding the Little Ice Age maximum. Quat. Sci. Rev. 98, 135–143.
Wooller, M.J., Francis, D., Fogel, M.L., Miller, G.H., Walker, I.R., Wolfe, A.P., 2004. Quantitative Paleotemperature estimates from delta O-18 of chironomid head capsules preserved in arctic lake sediments. J. Paleolimnol. 31, 267–274.
Young, N.E., Briner, J.P., Stewart, H.A.M., Axford, Y., Csatho, B., Rood, D.H., Finkel, R.C., 2011a. Response of Jakobshavn Isbræ, Greenland, to Holocene climate change. Geology 39, 131–134. http://dx.doi.org/10.1130/G31399.1.
Young, N.E., Briner, J.P., Axford, Y., Csatho, B., Babonis, G.S., Rood, D.H., Finkel, R.C., 2011b. Response of a marine-terminating Greenland outlet glacier to abrupt cooling 8200 and 9300 years ago. Geophys. Res. Lett. 38, L24701. http://dx.doi.org/10.1029/2011GL049639.
Young, N.E., Schaefer, J.M., Briner, J.P., Goehring, B.M., 2013a. A ^{10}Be production-rate calibration for the Arctic. J. Quat. Sci. 28, 515–526.
Young, N.E., Briner, J.P., Rood, D.H., Finkel, R.C., Corbett, L.B., Bierman, P.R., 2013b. Age of the Fjord Stade moraines in the Disko Bugt region, western Greenland, and the 9.3 and 8.2 ka cooling events. Quat. Sci. Rev. 60, 76–90. http://dx.doi.org/10.1016/j.quascirev.2012.09.028.